NAIRA VALLE DE CASTRO

THE INORGANIC CARBON SOURCE AND CONCENTRATION AFFECT GROWTH AND CENTRAL METABOLISM IN A MICROCYSTIN PRODUCER CYANOBACTERIA

Dissertation presented to the Universidade Federal de Viçosa, as part of the requirements of the Plant Physiology Graduate Program, to obtain the title of *Magister Scientiae*.

VIÇOSA
MINAS GERAIS-BRAZIL
2019

Ficha catalográfica preparada pela Biblioteca Central da Universidade Federal de Viçosa - Câmpus Viçosa

T
C355i
2019

Castro, Naira Valle de, 1994-
The inorganic carbon source and concentration affect growth and central metabolism in a microcystin producer cyanobacteria / Naira Valle de Castro. – Viçosa, MG, 2019.
viii, 61 f. : il. ; 29 cm.

Texto em inglês.
Orientador: Wagner Luiz Araújo.
Dissertação (mestrado) - Universidade Federal de Viçosa.
Referências bibliográficas: f. 43-55.

1. Cianobactéria. 2. Microcistinas. 3. Carbono.
I. Universidade Federal de Viçosa. Departamento de Biologia Vegetal. Programa de Pós-Graduação em Fisiologia Vegetal.
II. Título.

CDD 22. ed. 579.83

NAIRA VALLE DE CASTRO

THE INORGANIC CARBON SOURCE AND CONCENTRATION AFFECT GROWTH AND CENTRAL METABOLISM IN A MICROCYSTIN PRODUCER CYANOBACTERIA

Dissertation presented to the Universidade Federal de Viçosa, as part of the requirements of the Graduate Program in Plant Physiology, to obtain the title of *Magister Scientiae*.

APPROVED: July 31, 2019.

Diego Bonaldo Genuário

Adriano Nunes Nesi

Marcelo Gomes Marçal Vieira Vaz
(Co-adviser)

Wagner Luiz Araújo
(Advisor)

ACKNOWLEDGEMENTS

To my parents, Dinho and Inezinha, to my sister and brother, Mariah and Ian, for all the support and unconditional love, even distant.

To Professor Wagner, for all guidance, patience, wisdom, support and for believe in me. Without him this work would not be possible.

To Marcelo, whose orientations passed the academic environment and serve for life. For spending entire nights correcting my work, and giving it as much importance as if it was his. For being an incredible person, I will always remember you.

To Allan, who shared with me all the joys and burdens of this master's degree. For being with me in the nights in my project, for always being by my side and being a great company.

To all the incredible people who work with me in the laboratory, especially, Jean, Lidi, Rina, Regina, Jonas, Elias, Dora, Fran, Marcelle, Roberto and Ítalo, who made me happy at work, being big companies and for always helping me.

To my quinteto, for all the friendship and support, even distant.

The residents and former residents of the MinaMora republic, who made the republic a home.

To Rômulo, for love, patience and for being one of my greatest supporters.

To all professors of the Plant Physiology Graduate Program for the valuable teachings.

To the Universidade Federal de Viçosa and Plant Physiology Graduate Program, for the opportunity to develop of this work.

To CNPq, FAPEMIG and CAPES for the financial support of this study, making it possible.

To all the people who made this work possible and contributed in any way.

I am sincerely grateful, thank you.

SUMMARY

ABSTRACT

CASTRO, Naira Valle de, M.Sc., Universidade Federal de Viçosa, July, 2019. **The inorganic carbon source and concentration affect growth and central metabolism in a microcystin producer cyanobacteria.** Adviser: Wagner L. Araújo. Co-adviser: Marcelo Gomes Marçal Vieira Vaz.

Cyanobacteria, microorganisms belonging to the *Bacteria* domain, are widely distributed geographically, yet most genera are found in freshwater environments. Some cyanobacterial strains are able to produce toxins (cyanotoxins), like microcystins (MCs), that show hepatotoxic effect in animals. The genetic basis, chemical structure, and biosynthetic route as well as microcystin action in eukaryotic organisms have been deeply studied. However, it remains unknown which are the roles played by such compounds in the producing organism. Here, we tested the hypothesis that growth medium supplied with different concentrations of inorganic carbon (Ci) source promotes metabolic and physiological adjustments coupled with changes in MC production. To this end, the cyanobacterial strain Scytonemataceae CCM-UFV057 was cultured in different growth medium, (i) standard BG-11_0 (supplied with 0.02 $g \cdot L^{-1}$ of sodium carbonate), as control; (ii) BG-11_0 without Ci (T1); and (iii) BG-11_0 supplied with two concentrations of sodium bicarbonate, 0.016 $g \cdot L^{-1}$ (T2) and 1.6 $g \cdot L^{-1}$ (T3). Growth evaluation together with physiological and biochemical analysis as well as MC's quantification were carried out. Growth parameters of CCM-UFV057 were similar for all growth conditions. Both T1 and T2 lead to similar metabolic patterns, despite different responses in both photosynthetic and respiratory rates. The strain CCM-UFV057 was able to produce five MCs congeners, with the variants showing *m*/*z* of 540 and 1037 as the most abundant forms in all conditions. MCs production was highly influenced by Ci concentration, and T1 and T3 lead to the higher and lower MC concentration, respectively, indicating that low Ci concentrations somehow improve the MC production. Notably, the carbon source (carbonate *versus* bicarbonate) did not seems to affect MC production. Taken together, our data suggest that high amounts of MC

under low Ci conditions can contribute to the maintenance of photosynthetic rates, keeping both higher carbon assimilation rates and cellular homeostasis without growth impairments.

RESUMO

CASTRO, Naira Valle de, M.Sc., Universidade Federal de Viçosa, julho de 2019. **A fonte e a concentração de carbono inorgânico afetam o crescimento e o metabolismo central de uma cianobactéria produtora de microcistina.** Orientador: Wagner L. Araújo. Coorientador: Marcelo Gomes Marçal Vieira Vaz.

Cianobactérias são organismos pertecentes ao domínio *Bacteria*. Esses microorganismos são amplamente distribuídos, embora a maior parte dos gêneros seja encontra em ambientes de água doce. Algumas cianobactérias produzem toxinas (cianotoxinas), como as microcistinas (MCs), que apresentam efeito hepatotóxico em animais. Toda a base genética, estrutura química e rotas de biossíntese, assim como a ação da microcistina nos organismos eucariotos, já foi elucidada. Não obstante, não se sabe ainda quais são os papéis desses compostos no organismo que o produz. Neste estudo, testou-se a hipótese de que a linhagem Scytonemataceae CCM-UFV057 é capaz de crescer em meios com diferentes concentrações e fontes de carbono inorgânico modulando as quantidades de MC produzidas na célula. Para tanto, essa linhagem foi cultivada em meio BG-11_0, com 0,02 g.L^{-1} de carbonato de sódio, sendo o controle; em meio BG-11_0 sem fonte de carbono (T1); e em em meio BG-11_0 suplementado com duas concentrações de bicarbonato de sódio, 0,016 g.L^{-1} (T2) e 1,6 g.L^{-1} (T3). Análises de crescimento, fisiológicas, bioquímicas e de produção de MCs foram conduzidas. Os parâmetros de crescimento e cinéticos foram similares entre os tratamentos. As análises bioquímicas indicaram um padrão semelhante entre T1 e T2, embora tenham sido observadas diferenças nas taxas de fotossíntese e de respiração. Verificou-se também que a linhagem CCM-UFV057 produz cinco variantes de MC, dentre as quais, as variantes com *m*/*z* 540 e 1037 foram as mais abundantes nas condições testadas. Levando-se em consideração o conteúdo total de MC, T3 apresentou os menores valores ao passo que T1, os maiores, com valores semelhantes para o controle e T2. Tomados em conjunto, os resultados obtidos indicam que a quantidade de MC produzida pela linhagem CCM-UFV057 é modulada pelas concentrações de

carbono no meio, ao passo que a fonte de carbono utilizadas não impacta essa quantidade. Em suma, os resultados aqui apresentados sugerem que concentrações elevadas de MC produzidas sob baixa concentrações de carbono no meio contribuem, ao menos parcialmente, para a manutenção das taxas fotossintéticas e da homeostase celular sem prejuízos ao crescimento.

1. INTRODUCTION

Cyanobacteria are prokaryotic microorganisms belonging to the *Bacteria* domain capable to perform oxygenic photosynthesis. Some genera are also able to perform the biological nitrogen fixation (BNF) (Woese, 1987). Although these microorganisms form a phylogenetic coherent group (Giovannoni et al., 1988; Shi and Falkowski, 2008), they display great morphological diversity, ranging from unicellular (solitary or colonial) to filamentous (homocytous and heterocytous) morphotypes. Members of the phylum *Cyanobacteria* are widespread and present adaptations to colonize diverse habitats (Castenholz, 2001), yet the vast majority are found in freshwater environments (Woese, 1987).

Cultural eutrophication – i.e., the over-enrichment of surface waters with nutrients, primarily nitrogen (N) and phosphorus (P) – is frequently a key driver of cyanobacterial bloom formation (Watson S.B. et al., 1997; Smith V.H. et al., 1999). The incidence and intensity of cyanobacterial blooms are on the rise worldwide (de Figueiredo D.R. et al., 2004; O'Neil J.M. et al., 2012; Paerl H.W. & Otten T.G., 2016). The most important reason why cyanobacterial blooms are viewed as problematic is that they present a serious health threat because of the potent toxins (cyanotoxins) they might produce (Codd G.A. et al., 2005).

Cyanotoxins are characterized as bioactive substances, produced by several genera of cyanobacteria, which present a toxic effect on humans and other animals (Briand et al., 2016, 2008). Among the known cyanotoxins, microcystin (MC) is by far the most studied (Briand et al., 2016). This cyanotoxin is a cyclic heptapeptide, which has the basic structure D-Ala (1) - X (2) - D-MAsp (3) - Z (4) - Adda (5) - D-Glu (6) - Mdha (7), in which X and Z are the most variable groups (Sivonen and Jones, 1999). Whilst microcystin-LR refers to leucine and arginine at these positions (Sivonen and Jones, 1999), Adda is responsible for the toxicity of MC (Rinehart et al., 1994). The production of several MCs isoforms by a single strain is rather common and, to date, more than 250 microcystin structural variants have been described (Schuurmans et al., 2018).

Microcystins are synthesized by a non-ribosomal pathway mediated by enzymatic complexes including the Non-Ribosomal Peptide Synthesis (NRPS)

and Polyketide Synthases (PKS) (Tillett et al., 2000). All the genes required for the coding of these NRPS and PKS complexes as well as tailoring enzymes responsible for MC biosynthesis are in the same gene cluster denominated *mcy* (Tillett et al., 2000). Interestingly, this cluster is not found in the same way in all microcystin-producer cyanobacterial genera. Accordingly, variations can occur on the number of genes and transcriptional direction (Christiansen et al., 2003; Fewer et al., 2013; Rouhiainen et al., 2004; Rounge et al., 2009; Tillett et al., 2000).

The chemical structure (Botes et al., 1984), biosynthetic pathway and genetic organization (Dittmann et al., 1997, 1996; Neilan et al., 1999; Tillett et al., 2000) as well as the action of microcystins in eukaryotic organisms (de Figueiredo et al., 2004) have been elucidated during the last decades. Despite that the biological functions of this molecule on cyanobacterial cells and on overall metabolism as well as the reasons for its production remains unknown (Briand et al., 2016). Several hypothesis have been suggested, one of them being the influence of carbon concentrations on its production (Van De Waal et al., 2011); however, up to now, the function of MC in cyanobacterial cells has not been unequivocally proven.

In this context, the main goal of this work was to characterize the effect of carbon sources and concentrations on microcystins production, as well as on the physiological and metabolic responses of the strain Scytonemataceae CCM-UFV057, emphasizing the possible role played by microcystins on photosynthetic metabolism.

2. LITERATURE REVIEW

Cyanobacteria are microorganisms belonging to the *Bacteria* domain capable to perform oxygenic photosynthesis, and certain genera are also able to perform the biological nitrogen fixation (BNF) (Woese, 1987). Fossil studies and molecular evidences suggest that these organisms emerged about 3.5 billion years ago (Altermann and Kazmierczak, 2003; Schopf, 1993). Accordingly, as result of their metabolism, mainly due to atmospheric carbon fixation and BNF,

cyanobacteria are important agents in the biogeochemical cycles of carbon and nitrogen (Knoll, 2008).

Although these microorganisms form a phylogenetical coherent group (Giovannoni et al., 1988; Shi and Falkowski, 2008), they also display distinct morphologies, ranging from unicellular (solitary or colonial), to filamentous forms. The filamentous strains can be divided into homocytous, whose cells are similar regarding their morphologies, or heterocytous, that besides vegetative cells, also present differentiated cells, such as heterocytes (specialized cells for BNF) and akinetes (spore-like cells) (Flores and Herrero, 2009).

Cyanobacteria are widespread and present adaptations to colonize diverse habitats (Castenholz, 2001). Among the morphophysiological adaptations exhibited by cyanobacteria are include (i) hormogonia, filaments presenting gas vesicles-rich cells or gliding motile, enabling their dispersion; (ii) presence of high amounts of exopolysaccharide, which protects them against desiccation; and (iii) its basic nutritional requirements (CO_2, H_2O and light, mainly), among others (Castenholz, 2001; Rippka et al., 1979). This fact aside, the vast majority of cyanobacterial strains are found in freshwater environments, constituting an emergent problem when inhabiting water reservoirs for public supply, since some groups are commonly associated with blooms and cyanotoxin production (Paerl and Huisman, 2008).

Domestic and industrial effluents, agriculture activities (pesticides and fertilizers), and inadequate management of watersheds, all may be pointed out as the major causes of eutrophication (Vasconcelos V., 2006). The consequences of eutrophication are usually associated with low water quality, such as the production of large phytoplankton blooms (Vasconcelos V., 2006). This phenomenon has been recognized as a global problem in sustaining lake ecosystems and human health (Carmichael W.W, 2001), because many cyanobacteria species and strains are able to produce bioactive compounds with toxic properties (Vasconcelos V., 2006). These toxins can cause death not only to aquatic organisms that come in direct contact with them but also to livestock, domestic animals, waterfowl and humans (Vasconcelos V., 2006).

Cyanotoxins are bioactive compounds, produced by several cyanobacterial genera, which display toxic effect on humans and other animals (Briand et al., 2016). These substances have been described according to their chemical classes or their biological effects, being classified as: hepatotoxins (microcystins and nodularins), neurotoxins (saxitoxins, anatoxin-a), cytotoxins (cylindrospermopsin) (Carmichael, 2001), among others. To date, microcystin, which was discovered in 1959 in a culture of *Microcystis aeruginosa* (Bishop et al., 1959), is by far the most studied (Briand et al., 2016) among the known cyanotoxins. Although it was named in reference to the genus *Microcystis*, in which it was initially characterized, it is currently known that other genera, including *Anabaena*-like (*Cuspidothrix, Dolichospermum, Macrospermum, Sphaerospermopsis), Aphanizomenon, Planktothrix, Anabaenopsis, Cylindrospermopsis, Fischerella, Gloeotrichia, Gomphosphaeria, Hapalosiphon, Nodularia, Nostoc*-like (*Aliinostoc* and *Nostoc), Oscillatoria, Phormidium, Pseudanabaena* and *Synechococcus* (Preece et al., 2017), are capable of producing MC variants. It is important to highlight that the genera mentioned above are morphologically distinct, including unicellular, homocytous and heterocytous morphotypes, which present great variation regarding the MC variants that are produced (Schuurmans et al., 2018).

Chemically, microcystins are heptapeptides of cyclic structure, which have the classical structure (1) - X (2) - D-MAsp (3) - Z (4) - Adda (5) - D-Glu (6) - Mdha (7), in which X and Z are the most variable groups (for example, microcystin - LR refers to leucine and arginine at these positions) (Sivonen and Jones, 1999). The Adda residue is a 3-amino-9-methoxy-2-6,8-trimethyl-10-phenyl-4,6-decadienoic acid, responsible for the toxicity of microcystin (Rinehart et al., 1994). The production of several MC isoforms by a single cyanobacterial strain is rather common and, to date, more than 250 microcystin structural variants have been described (Schuurmans et al., 2018).

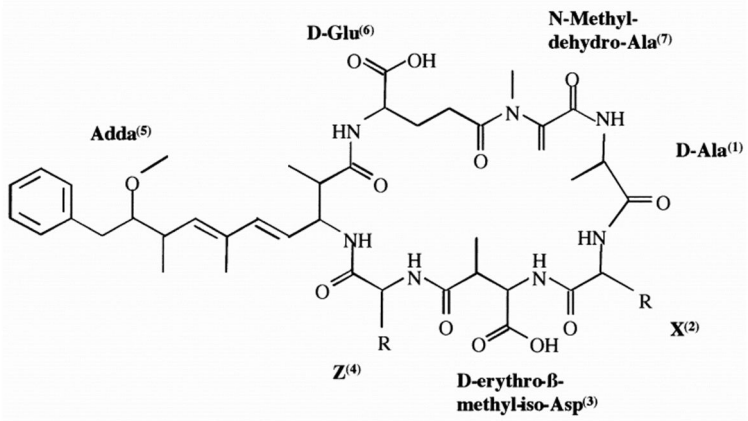

Figure 1. General structure of the microcystin.
Source: Tillett et al., 2000.

Microcystins have an inhibitory action on serine/threonine phosphatase, especially those from type 1 (PP1) and type 2A (PP2A) (de Figueiredo et al., 2004). This action occurs by the entrance of the microcystin molecule into the hepatocytes *via* active transport by Organic Anion Transporting Polypeptides (OATPs) (Hagenbuch and Gui, 2008; Kalliokoski and Niemi, 2009). The lethal dose among the MC variants, considering the mice body mass, ranges from 600 $\mu g \cdot kg^{-1}$ in the case of microcystin-RR (Watanabe et al., 1988) to 50 $\mu g \cdot kg^{-1}$, in the case of microcystin-LR, which is the most common isoform (Krishnamurthy et al., 1986).

Microcystins are synthesized by non-ribosomal enzymes, mediated by enzymatic complexes such as Non-Ribosomal Peptide Synthetase (NRPS) and Polyketide Synthases (PKS) (Shishido et al., 2013). The NRPS complex is responsible for the recognition and incorporation of amino acid residues during the elongation and formation of the peptide (Shishido et al., 2013). This complex basically has domains of condensation (C), adenylation (A) and a peptidyl carrier protein (PCP) (Shishido et al., 2013). The adenylation domain is responsible for the selection and activation of amino acids in the form of aminoacyl adenylates (Stachelhaus et al., 1999). It is followed by the PCP domains, in which the activated amino acid is found, and by the domain of condensation that binds two adjacent amino acids residues (Finking and Marahiel, 2004). In addition, auxiliary enzymes are present playing roles during epimerization, cyclization, N-

methylation, formylation and reduction of amino acids (Sieber and Marahiel, 2005; Walsh et al., 2001).

All the genes required for the coding of these NRPS and PKS complexes and for MC biosynthesis are in the same gene cluster called *mcy* (Tillett et al., 2000). In *M. aeruginosa* PCC7806, this cluster contains 10 genes (*mcy*A-*mcy*J), organized into two bidirectionally transcribed operons, namely *mcy*A-C and *mcy*D-J (Dittmann and Börner, 2005).

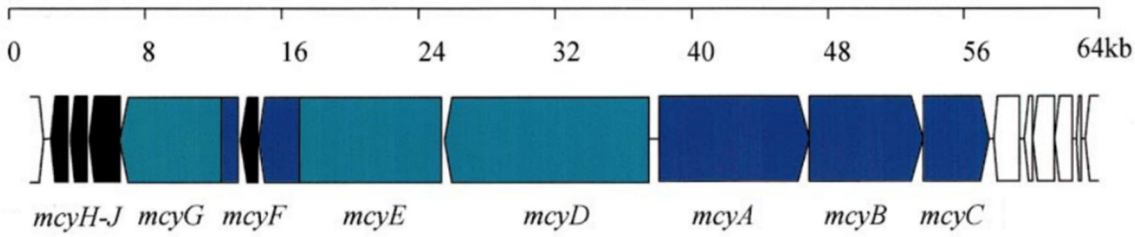

Figure 2. Organization of the gene cluster for microcystin biosynthesis in *M. aeruginosa* PCC7806. The direction of transcriptions and relative sizes are indicated. ORF's containing NRPS and PKS are in dark and light blue, respectively. ORF's with putative microcystin tailoring function are indicated in black. Non-microcystin synthetase ORF's are show in white.
Source: Tillett et al., 2000.

The largest of the two operons, *mcy*D-J, encodes a modular PKS (McyD), two hybrid enzymes containing NRPS and PKS modules (McyE and McyG), as well as complementary enzymes (McyJ, F and I) and toxin transporter (McyH), whereas the smallest operon, *mcy*A-C encodes three NRPS (McyA-C) (Dittmann and Börner, 2005). It is important to mention that the organization of *mcy* cluster is not the same for all cyanobacterial genera. Clusters with variation in the number of genes (7,8,9,11) have already been described (Christiansen et al., 2003; Fewer et al., 2013; Rouhiainen et al., 2004; Rounge et al., 2009; Tillett et al., 2000). For instance, the toxic strain *Nostoc* sp. 152 has a differential gene, *mcy*L, and lacks the *mcy*I and *mcy*J genes, all three genes encoding for complementary enzymes (Fewer et al., 2013). In addition, in some strains, such as *Planktothrix agardhii* NIVA-CYA 98, the transcription is not bidirectional, being initiated unidirectionally by the *mcy*D gene (Rounge et al., 2009).

The chemical structure (Botes et al., 1984), biosynthetic pathway and genetic organization (Dittmann et al., 1997, 1996; Neilan et al., 1999; Tillett et al.,

2000) as well as the action of microcystins in eukaryotic organisms (de Figueiredo et al., 2004) have been unequivocally demonstrated during the last decades. Notwithstanding, the biological function of this molecule on cyanobacteria and the reason(s) for its production are still unknown (Briand et al., 2016). Several theories are currently available trying to associated the synthesis of microcystins to light adaptation and oxidative stress (LeBlanc Renaud et al., 2011; Meissner et al., 2014; Zilliges et al., 2011), temperature (Gao et al., 2011; O'Neil et al., 2012), pH values (Schatz et al., 2005; van der Westhuizen et al., 1988), action against herbivory (Jang et al., 2003; Müller-Navarra et al., 2000; Watson, 2003; Zhen and Kong, 2012), nutrients acquisition (Davis et al., 2009; Jähnichen et al., 2001; Jährlichen et al., 2007; Yu et al., 2014), or a set of these variables (Geada et al., 2017). However, the exact function of MC in cyanobacterial cells as well as the biotic and abiotic stimuli driven its production has not yet been proven.

A possible relationship between MC biosynthesis and the presence of low concentrations of inorganic carbon has been demonstrated (Van De Waal et al., 2011). Two *Microcystis* strains, one toxic and one non-toxic, were grown at low CO_2 concentrations (200 ppm). The toxin-producing strain, grown in monoculture, showed higher growth rate, higher population density and greater ability to remove inorganic carbon from the medium. When in co-cultivation, the toxic strain was dominant over the non-toxic one, inhibiting its growth. The same behavior was observed in co-cultivation using a microcystin-producing *Microcystis* strain and its mutant, unable to produce the toxin (Van De Waal et al., 2011). Thus, these results allowed these authors to postulate that the production of MC may affects the cellular ability to utilize inorganic carbon.

Similar results were found by Sandrini et al. (2016), which showed the differential growth of *Microcystis* strains when grown in media with different CO_2 concentrations. These authors used two strains carrying the sodium-dependent bicarbonate transporters, BicA and SbtA, which differed only by MC production, being one a producer and the other not. At low CO_2 concentration (100 ppm), the microcystin-producing strain dominated the population in such way that the

growth of the non-producer was inhibited. By sharp contrast, in high CO_2 concentrations (1000 ppm), the nontoxic lineage predominated (Sandrini et al., 2016).

It is also known that MC can bind covalently to many proteins (Zilliges et al., 2011). In addition, toxic and mutant strains for MC production accumulate different isoforms of the same proteins (Zilliges et al., 2011). According to these authors, microcystin can bind to the major subunit of RubisCO, possibly increasing its stability. Furthermore, the genes related to small and large subunit of RubisCO are differentially expressed between mutants deficient for MC production compared to the wild type, being repressed more than two fold in mutant strains (Zilliges et al., 2011).

Taken together, here we hypothesized that: (i) low inorganic carbon (Ci) concentrations increases MC production and (ii) microcystin synthesis is stimulated at low concentrations of Ci, given that this molecule may play an important role in Ci absorption and/or assimilation, positively impacting overall photosynthesis. To test this hypothesis, we used the filamentous heterocytous cyanobacteria Scytonemataceae CCM-UFV057, a microcystin-producer strain, and cultivated it in media supplied with different sources and concentrations of Ci.

The work presented here is largely focused on understanding how the filamentous heterocytous cyanobacterial strain Scytonemataceae CCM-UFV057, a microcystin-producer, can cope with different sources and concentrations of Ci. That being said, the aims of this work were: *(i)* to obtain a comprehensive metabolic and physiological overview of how and to which extent the strain Scytonemataceae CCM-UFV057 is able to deal with low and high Ci concentrations; *(ii)* to characterize the possible action of microcystins on the physiological and metabolic responses of the CCM-UFV057 strain when cultured in different sources/concentrations of inorganic carbon; and *(iii)* to evaluate and quantify the production of microcystins at different growth periods and in a complete day (24 hours) in the middle of logarithmic and stationary phases, considering the growth in different culture media. To reach these goals several

different but complementary experimental approaches were undertaken and the results obtained are further discussed in the context of the current models of cyanobacterial responses to Ci and the impact microcystin has on it.

3. MATERIAL AND METHODS

3.1 Strain Selection

It is known that both toxin-producing and non-toxin producing genotypes of cyanobacteria coexist in nature. However, it is not possible to distinguish them based only on morphological characteristics (Carmichael and Gorham, 1981). Thus, the screening for strains able to produce cyanotoxins has been conducted, based on molecular/chemical approaches (Silva et al., 2014), in all cyanobacterial strains maintained at the Collection of Cyanobacteria and Microalgae at the Universidade Federal de Viçosa (CCM–UFV), by means of PCR analysis (molecular evaluation), aiming to select strains with genetic potential for microcystin production.

Briefly, total genomic DNA was extracted from a 2-3 weeks-old cultures of all strains available at CCM-UFV, using the UltraClean® Microbial DNA Isolation Kit (MoBio, Carlsbad, CA). For the molecular screening of potential microcystin-producers, three synthetase genes were selected: partial regions of *mcy*D (~818 bp) and *mcy*E (~809 bp) were amplified using the specific primers designed by Rantala et al. (2004), while partial *mcy*G (~534 bp) sequence was amplified using the primer set described by Fewer et al. (2007). The PCR amplifications were performed as described by Genuário et al. (2013).

After PCR evaluation and sequencing, the strains which showed positive results for the three screened genes (*Nostoc* sp. CCM-UFV010, *Nostoc* sp. CCM-UFV019, *Fischerella* sp. CCM-UFV026, *Fischerella* sp. CCM-UFV036, and Scytonemataceae CCM-UFV057) were also evaluated by LC-MS, to ensure the production of MC. Taken together, three out of the five strains were confirmed as MC producers: *Fischerella* sp. CCM-UFV026, *Fischerella* sp. CCM-UFV036, and Scytonemataceae CCM-UFV057 (hereafter CCM-UFV057), being the last one chosen for this study.

3.2 Growth Conditions

From the stock culture, the strain CCM-UFV057 was cultivated in an increasing scale for the production of biomass in Erlenmeyer flasks (125, 250, 500, 750 and 1,000 mL) filled with BG-11_0 medium (Rippka et al., 1979) without nitrogen, since this strain can fix atmospheric nitrogen. The strain was cultured successively at intervals of 7 days until sufficient biomass was obtained for the experiments. At each interval, the biomass was centrifuged (10,000 × *g*, 10 minutes, 4 ℃), then the supernatant was discarded and the pellet re-inoculated into fresh culture medium. During these steps, the cyanobacterial strain was grown in orbital shaker with constant agitation of 100 rpm, at a temperature of 23 ± 2 ℃, under light irradiance of 95 μmol photons·m^{-2}·s^{-1}, provided by 20 W LED lamps (Light Emitter Diode) (Kian, Led Tube, China) and photoperiod of 16:8 h (light:dark). The light intensity was selected after evaluations of the photosynthetic response at different irradiances by Clark's electrode.

Briefly, the experiments were conducted in Erlenmeyer flasks containing the appropriated culture medium. The BG-11_0 medium (BG-11 without nitrogen source) was used as control. Three treatments were also conducted: (1) BG-11_0 medium without any carbon source supplementation (T1); BG-11_0 in which the Na_2CO_3 (original carbon source) was replaced by sodium bicarbonate ($NaHCO_3$), in two concentrations: (2) 0.016 g·L^{-1}, which is the equimolar amount of carbon used in the standard BG-11_0 medium (T2); and (3) 1.6 g·L^{-1} (T3). This concentrations of carbon were defined based on previously experiments (data no shown). The experiments were conducted under the same photoautotrophic conditions as described above. The initial amount of biomass inoculated into each Erlenmeyer flaks was sufficient to reach OD_{750nm} of ~ 0.1.

3.3 Growth Curves

Growth curves were conducted to evaluate the growth phases of each treatment: BG-11_0 without carbon source, BG-11_0 supplemented with 0.016 g·L^{-1} ($NaHCO_3$) and BG-11_0 supplemented with 1.6 g·L^{-1} ($NaHCO_3$), and the control medium. The curves were performed with four replicates, in Erlenmeyer flasks (125 mL volume) containing 60 mL of the appropriated culture medium, and were

conducted during 15 days, with daily measurements of cellular growth by determination of optical density, OD_{750nm} (UV-Vis Spectrophotometer, UV mini 1240, Shimadzu). The experiment was conducted under the same photoautotrophic conditions as described above.

After the determination of the growth phases, new curves were conducted aiming to analyze a 24-hour cycle in the middle-logarithmic and in the early-stationary phases. During the 24-hours cycles, samples were taken every 6 hours (0, 6, 12, 18 and 24 h, totalizing five sampling points). The biomass collected were used to determine the cell weight, as well as sampled for biochemical and toxin analyzes, as described below. For this second round of growth curves Erlenmeyer flasks (250 mL volume) containing 100 mL of the appropriated culture medium were used. The curves were performed with four replicates and were conducted under the same photoautotrophic conditions as described above.

In this last experiment, growth was assessed by determination of absorbance (OD_{750nm}) and ash-free dry mass. For the dry mass determination, aluminum foil crucibles were previously oven dried at 60 ℃ for 24 h (constant weight) and then were weighed. To the crucibles were added 10 mL of properly homogenized cell suspension. The biomass was then dried at 60 ℃ for 24 h and weighed. The dry mass was obtained by subtracting the weight of the crucibles with and without biomass. In addition, ash-free dry biomass was also evaluated. The aluminum foil crucibles containing dry biomass were packed in porcelain crucibles, which were submitted to calcination under muffle oven at 550 ℃ for two hours. The ash-free dry mass was obtained by subtracting the biomass value by the ash mass present in the crucibles after calcination. In addition to growth, the variation of pH values was also tracked along the two 24-hour cycles.

3.4 Microcystin Quantification

The extracts for the microcystin analyzes were obtained from lyophilized biomass (approximately 10 mg). The freeze-dried cells were subjected to mechanical disruption, using glass beads (Ø 3 mm) and 100 % methanol. This suspension was vortexed for 2 minutes and then centrifuged at 9,000 × *g* for 5 minutes at 4 ℃. The supernatant was collected, evaporated at 40 ℃ and the

extract kept at -20 ℃ until further analysis (Silva-Stenico et al., 2011, 2009). The dried extracts were resuspended in 1 mL of 100 % methanol and filtered (Millipore System, Ø 0.22 µm). Microcystin analyzes were performed in a Mass Spectrometer (Agilent 6410 Triple Quadrupole LC-MS equipped with Agilent 1200 Series Binary Pump SL and Agilent 1200 Autosampler) (Agilent Technologies Inc., Santa Clara, CA, USA). In the present study, the molecular ion search was performed in a range of 100 to 1,800 Da.

3.5 Photosynthesis and Respiration

Photosynthesis and respiration analyzes were carried out using the Clark electrode (Hansatech). Briefly, the instrument was calibrated using sodium dithionite to set 0 % saturation, and after washed with distilled water. Then, 2 mL of culture with OD_{750nm} = 0.8 was inoculated in the electrode chamber and curves of oxygen consumption and evolution, in response to photosynthetically active radiation (PAR), were performed at 25 °C by increasing in ten steps of five minutes the PAR intensities from 0 to 250 µmol photons $m^{-2} \cdot s^{-1}$.

Four replicates were collected every six hours during 24 hours in the log and stationary phases. A concentrated biomass, with total volume of 2 mL, OD_{750nm} of 0.8, were preconditioned for 20 minutes in the dark. Then, the biomass was introduced into the electrode chamber to measure photosynthesis. To do so, the aliquot within the chamber were maintained in the dark for seven minutes, then it was kept during five minutes in the intensities of 30 and 60 µmol photons m^{-2} s^{-1}, and ten minutes in the intensities of 95 and 125 µmol photons m $^{-2}$ s^{-1}, which correspond to the light intensity in which it was cultivated and the intensity of saturation light, respectively. The same sample was placed in the dark for 30 minutes for respiration analysis.

3.6 Biochemical Analysis

The samples (performing 5 sampling points) collected during the 24-hour cycles in the logarithmic and stationary phases were used for biochemical analysis. A total of 90 mL of homogenized biomass was collected and centrifuged at 13,500 × *g* for 10 minutes at 4 ℃. The supernatant was discarded and the

pellet frozen in liquid nitrogen, being then lyophilized and weighed. The lyophilized material was stored in a desiccator at -20 ℃ for further analysis.

For methanolic extraction, a known amount of lyophilized biomass was mixed with 700 µL of methanol (100 %) and heated at 80 ℃ for 20 minutes under stirring at 500 rpm. The methanolic extract was then centrifuged at 13,500 × *g* for 10 minutes at 4 ℃, and the supernatant was transferred to a new microtube (1.5 mL volume). The pellet was used for total soluble proteins and glycogen extraction, while the supernatant was used to quantify chlorophyll *a* and amino acids. Thus, 100 µL of the supernatant, plus 100 µL of methanol were used for quantification of chlorophyll *a*, by determination of optical densities at OD_{653nm} and OD_{666nm} (Microplate reader, Versa max, Molecular Devices) (Porra et al., 1989). To the residual volume were, sequentially, added 375 µL of chloroform and 750 µL of water. This new extract was centrifuged at 13,500 × *g* for 10 minutes at 4 ℃, leading to the formation of two very characteristic phases: one aqueous (polar, upper) and other, organic (apolar, lower). The aqueous phase, in which the metabolites of interest are found, were collected and transferred to another new microtube (1.5 mL volume) for amino acids quantification. To this aim, 350 µL of this aqueous phase was concentrated at speed vacuum (Concentrator plus, Eppendorf) and resuspended in 80 µL of ultra-pure water H_2O (Mili-Q®). For amino acids quantification, a total of 50 µL was transferred to a 96-wells microplate, being supplemented with 50 µL sodium citrate buffer (1 M, pH 5.2) + ascorbate 0.02%, as well as 100 µL of ninhydrin. The microplate was sealed and heated at 95 ℃ for 20 minutes, to be read at 570 nm (Microplate reader, Versa max, Molecular Devices) (Cross et al., 2006).

The pellet was washed with 1,000 µL of ethanol (70 %), treated with NaOH (0.1 M) and heated for one hour at 95 ℃ for protein extraction. Then was added at a microplate 250 µL of Bradford (Bio-Rad Protein Assay Dye Reagent Concentrate) and read at 595 nm (Microplate reader, Versa max, Molecular Devices) (Bradford, 1976). The rest of the pellet was neutralized with acetic acid (1 M) for glycogen quantification, at 340nm (Fernie et al., 2001).

3.7 Phycobiliproteins quantification

For phycobiliprotein (PBP) extraction and quantification samples were collected at middle of the day, in the logarithmic and stationary phases. A total of 90 mL of homogenized biomass was collected and centrifuged at 13,500 × *g* for 10 minutes at 4 ℃. The supernatant was discarded and the pellet frozen in liquid nitrogen, being then lyophilized and weighed. Approximated 25 mg of the lyophilized material were submitted to fragmentation in a tissue-lyzer (Retsch, MM400) and then used for the analysis.

The PBP extraction was carried out by incubating the biomass at 4 ℃, during 10 minutes, with 2 mL of lysis buffer (23% sucrose (*w*/*v*), 1 mM PMSF, 1.5 mM EDTA and 10 mM Tris–HCl (pH 8.0)). After incubation, the samples were homogenized in a vortex mixer (IKA® Vortex Genius3) three times at the highest speed for 1 minutes, with 1 minute's interval on ice. The cell debris were discarded after centrifuging at 3,300 × *g* for 10 minutes at 4 ℃. The supernatant was collected and centrifuged at 12,000 × *g* for 40 minutes at 4 ℃ (Centurion Scientific K3 Series); then, the coloured supernatant was collected. From this supernatant, 200 µL were used for quantification of phycocyanin, allophycocyanin and phycoerythrin by determination of optical density at OD_{565nm}, OD_{620nm} and OD_{650nm}, respectively (Microplate reader, Versa max, Molecular Devices) (de Marsac and Houmard, 1988).

3.8 Experimental Design

The experiments were conducted in a completely randomized design. All results obtained were submitted to analysis of variance (ANOVA), the means of the same treatment in different collection points and the means of different treatments at the same culture point were compared by Tukey test at 5% of probability, using the software Statistica.lnk.

4. RESULTS

4.1 Differential growth of a microcystin producer cyanobacteria in response to Ci levels

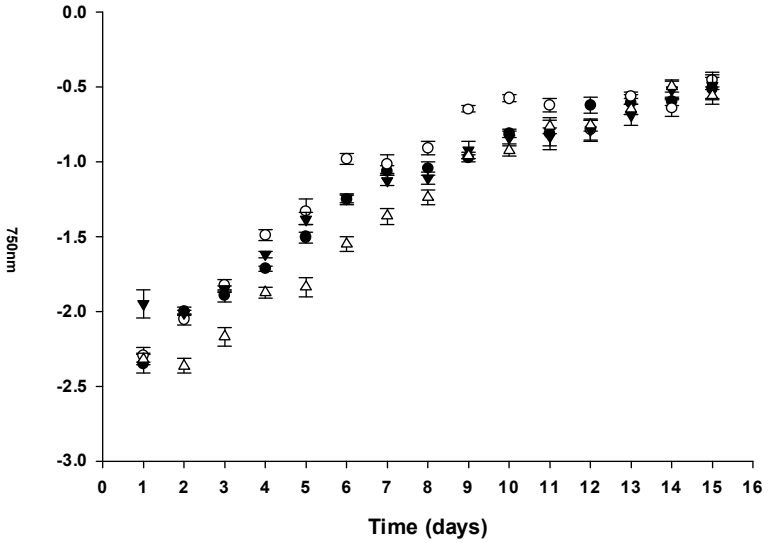

Figure 3. Growth curves based on optical density measurements (OD_{750nm}). Growth was monitored at 24 hours' intervals during 15 days. Growth curves of all treatments. Treatments: Control (black circles): Standard BG-11_0 culture medium with 0.02 g·L^{-1} of sodium carbonate; T1 (white circles): BG-11_0 culture medium without any carbon source; T2 (black triangles): BG-11_0 culture medium with 0.016 g·L^{-1} of sodium bicarbonate; T3 (white triangles): BG-11_0 culture medium with 1.6 g·L^{-1} of sodium bicarbonate. Values represent trend curves obtained from means ± standard error (n = 4). For statistical results, please see Table S1 (Supplemental data).

Growth curves obtained by means of optical density measurement (OD_{750nm}) presented similar patterns (Figure 3). Lag phases were absent and the strain CCM-UFV057 reached the stationary phase on the 10^{th} day, regardless the growth condition (Figure 3). The treatment without exogenous carbon source (T1), showed a tendency to present higher values of OD over the days of cultivation (Supplemental Figure 1A and 1C). However, from the 10^{th} day, beginning of the stationary phase, up to the end of the growth curves, no difference among the treatments was observed (Supplemental Figure 1A). Both Control and T2 had similar density values throughout the days (Supplemental Figure 1B and 1D), while T3 had the lower values compared to the others (Supplemental Figure 1E).

Table 1. Values of maximum growth rate (μ_{max}) and generation time (*Gt*).

Treatments	μ_{max}	*Gt* (hours)
Control	0.188 ± 0.004^{b}	88.338 ± 1.858^{a}
T1	0.263 ± 0.009^{a}	63.410 ± 2.390^{b}
T2	0.199 ± 0.013^{b}	84.464 ± 5.042^{ab}
T3	0.195 ± 0.021^{b}	87.968 ± 9.239^{a}

Values are presented as means ± standard error (n = 4). Means followed by the same letter for an individual parameter do not differ by 5% of probability (Tukey's test).

From the growth curves (Figure 3), kinetics parameters were also obtained (Table 1) and values of μ_{max} and generation time (*Gt*) corroborate with the slight differences found in the growth curves (Figure 3). T1 (BG-11_0 without any carbon source) showed the highest growth rate (μ_{max} = 0.26), as well as the shortest generation time (*Gt* = 63.41 h) (Table 1). For the other treatments, no statistical differences were observed for μ_{max}. T2 (BG-11_0 with 0.016 $g \cdot L^{-1}$ of sodium bicarbonate) presented a slightly lower generation time (84.46 h) than the control (88.33 h) and T3, the treatment with more carbon (87.96 h) (Table 1).

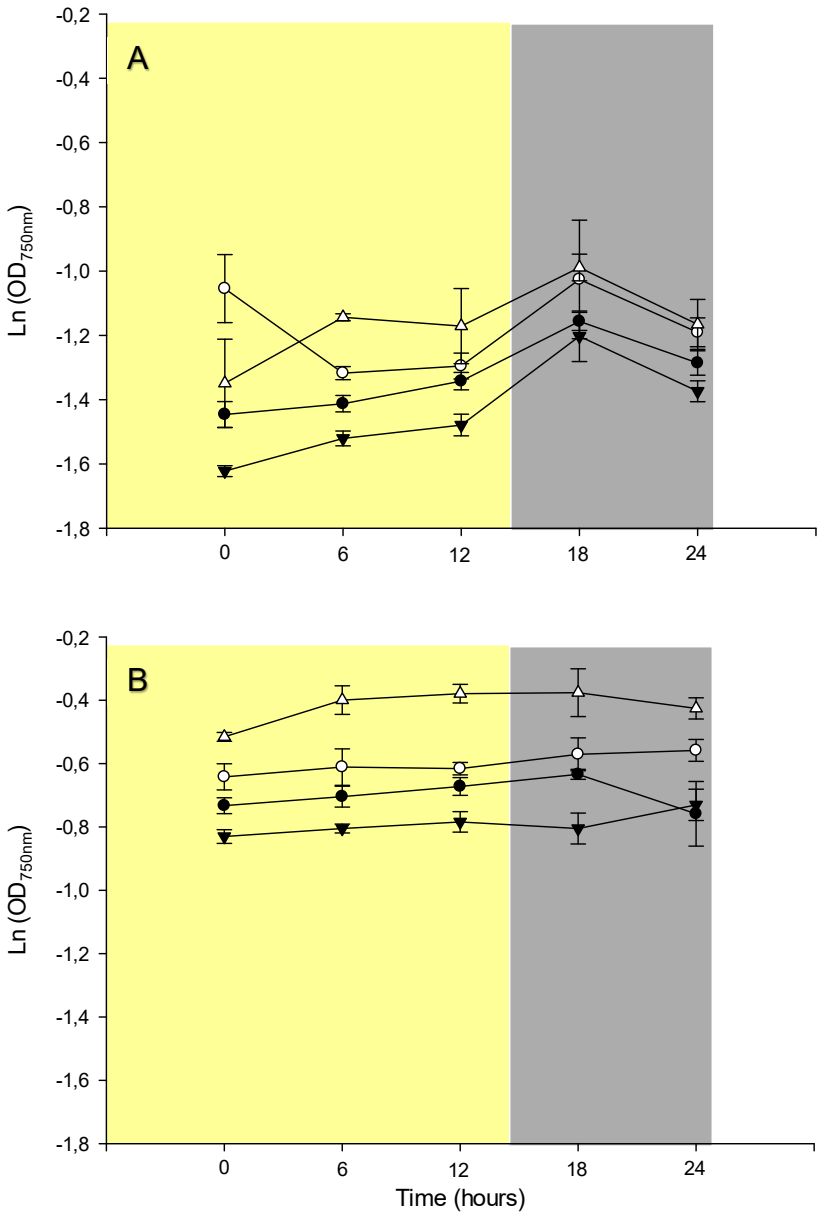

Figure 4. Growth curves based on optical density measurements (OD_{750nm}). Growth was monitored at 6 hours' intervals by optical density analysis during 24 hours. **(A)** Log phase; **(B)** Stationary phase. Treatments: Control (black circles): Standard BG-11_0 culture medium with 0.02 $g \cdot L^{-1}$ of sodium carbonate; T1 (white circles): BG-11_0 culture medium without any carbon source; T2 (black triangles): BG-11_0 culture medium with 0.016 $g \cdot L^{-1}$ of sodium bicarbonate; T3 (white triangles): BG-11_0 culture medium with 1.6 $g \cdot L^{-1}$ of sodium bicarbonate. Values are presented as means ± standard error (n=4). For statistical results, please see table S2 (Supplemental data).

Growth measurements conducted during a 24-hours period at both, logarithmic and stationary phases, by means of optical density and ash-free dry mass are presented in Figures 4 and 5, respectively. Based on the optical densities (OD), all treatments had similar patterns throughout the 24 hours and

also within the two phases. In the log phase (Figure 4A) the treatments begun with clear differences among them, in which T1 had the highest OD while T2 the lower one. All the treatments have a tendency of variation along the light phase (0-16 hours). However, at the end of the day (24 h), they showed similar OD (Figure 4A). It is important to mention that within the log phase, the treatments control and T2 presented differences in their OD values throughout the day, showing a very prominent peak in the evening, early night (18h). The other treatments displayed the same trend, but without statistical difference (Figure 4A).

In the stationary phase (Figure 4B), the treatment T3, in which the carbon concentration is higher, lead to the highest OD values, regardless the sampling point, followed by the treatment without carbon (T1) (Figure 4B). The treatment T2 showed the lowest OD values (Figure 4B). There were no significant changes in the OD values for all the treatments throughout the 24 h interval in the stationary phase (Figure 4B).

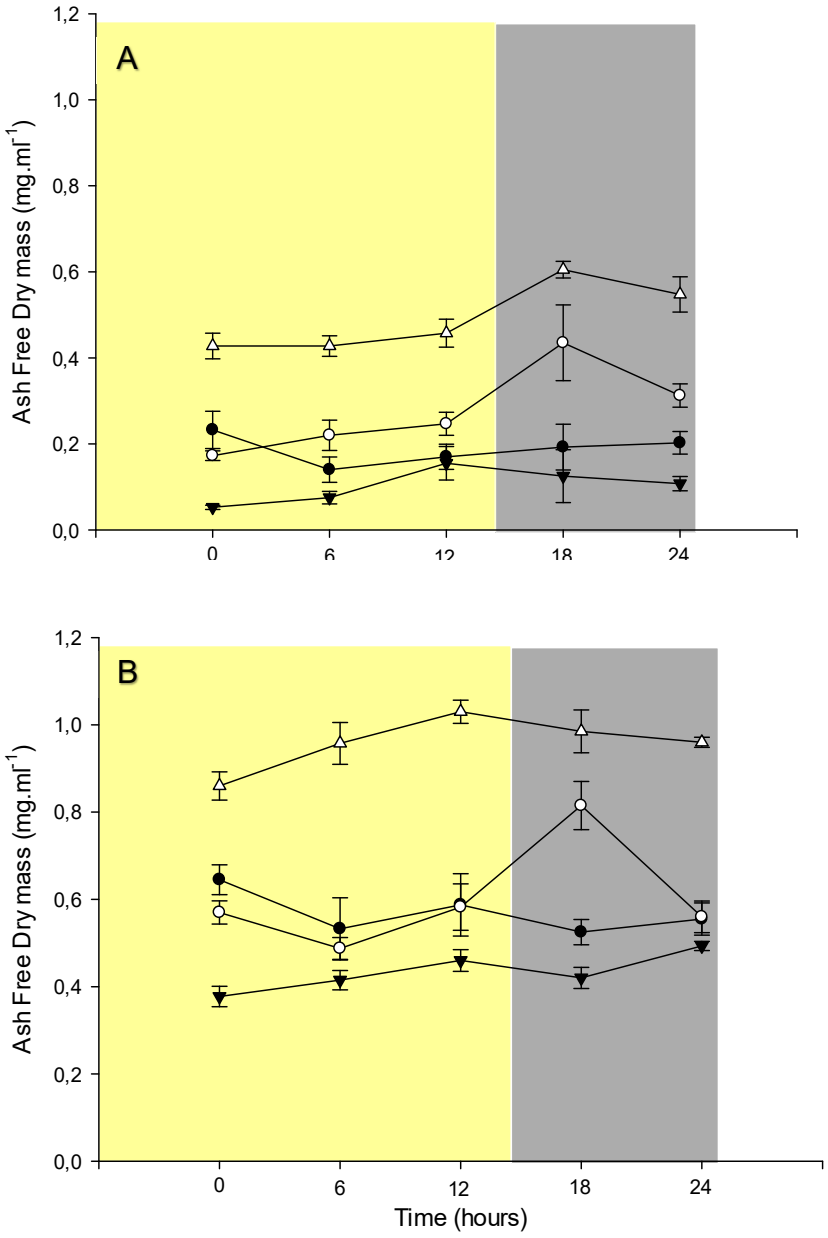

Figure 5. Growth curves based on ash-free dry mass. Growth was monitored at 6 hours' intervals by ash free dry mass analysis during 24 hours. **(A)** Log phase; **(B)** Stationary phase. Treatments: Control (black circles): Standard BG-11_0 culture medium with 0.02 g·L^{-1} of sodium carbonate; T1 (white circles): BG-11_0 culture medium without any carbon source; T2 (black triangles): BG-11_0 culture medium with 0.016 g·L^{-1} of sodium bicarbonate; T3 (white triangles): BG-11_0 culture medium with 1.6 g·L^{-1} of sodium bicarbonate. Values are presented as means ± standard error (n=4). For statistical results, please see table S3 (Supplemental data).

Given the growth measurements based on ash-free dry mass, it was possible to verify an increase in biomass, within a specific treatment along the day, in both log and stationary phases (Figure 5). T3 (higher Ci concentration) yielded the greater biomass values, compared to the other treatments in both

growth phases (Figure 5). The other treatments lead to very similar behavior along the day, excepted for the T1 (no Ci source), which showed a peak in both phases at 18 hours (Figure 5).

4.4 Microcystin quantification

4.4.1 Total content of microcystin

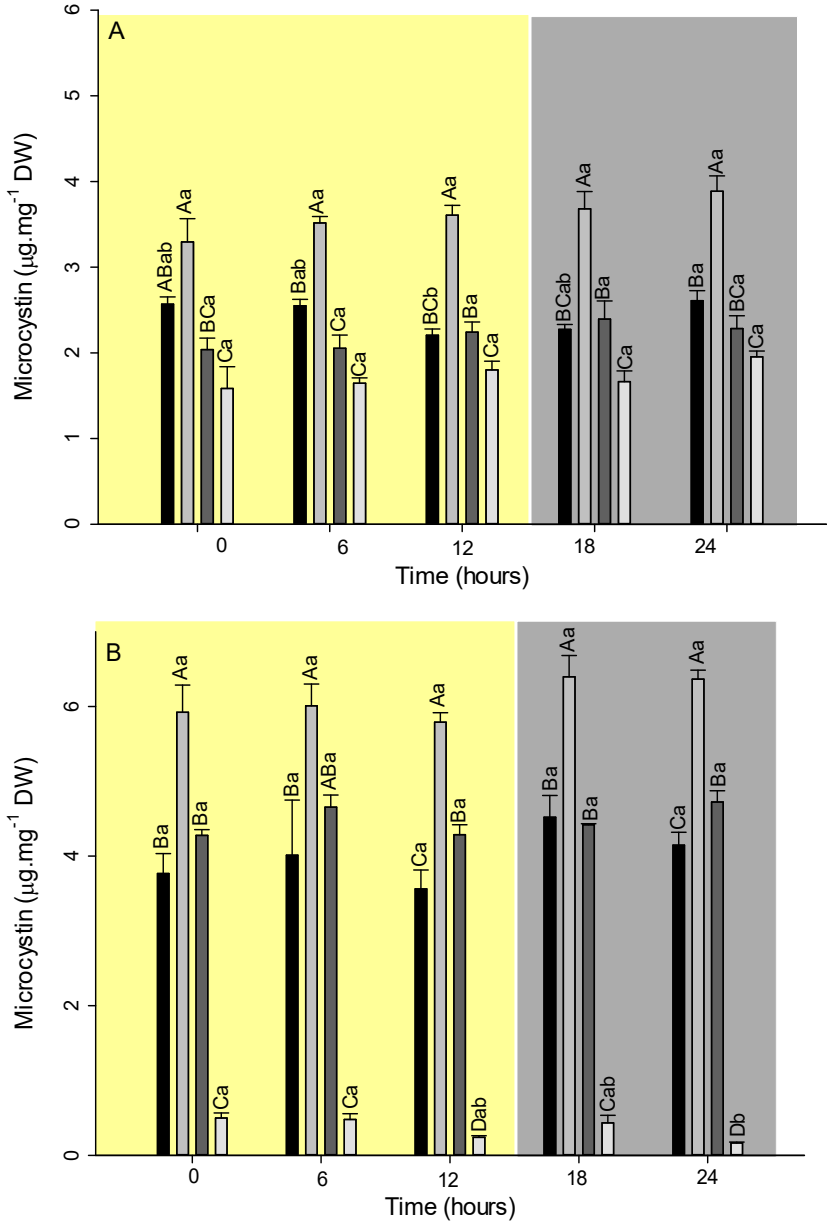

Figure 6. Variation in the total microcystin content in two growth phases. The microcystin content was collected at 6 hours' intervals during 24 hours and analyzed by LC-MS. **(A)** Log phase; **(B)** Stationary phase. Treatments: Control (black bars): BG-11_0 culture medium supplied with 0.02 g·L^{-1} of sodium carbonate; T1 (light grey bars): BG-11_0 culture medium without carbon source carbon; T2 (dark grey bars): BG-11_0 medium with 0.016 g·L^{-1} of sodium bicarbonate; T3 (lighter grey bars) $BG11_0$ medium with 1.6 g.L^{-1} of sodium bicarbonate. Values are presented as

means ± error (n=4). Different letters represent average values that were judged to be statistically different ($P < 0.05$, Tukey test). Capital letters represent statistical differences between the treatments, and lower-case letters demonstrate statistical differences along time.

Overall, the total content of microcystin was almost stable over the 24 hours' interval, in both growth phases and regardless the treatment. However, among the treatments, significant differences were observed for the total content of MC (Figure 6). Regardless the growth phase, the T1 (without inorganic carbon supplementation) lead to the higher values of total microcystin. In an opposite way, the T3, which was supplied with the highest inorganic carbon concentration, presented the lowest MC contents (Figure 6). It is equally important to mention that the biomass harvested in the stationary phase exhibited greater MC concentrations than those from logarithmic phase. The only exception was for the T3, which a decreased microcystin concentration was observed.

4.4.2 Microcystin variants content

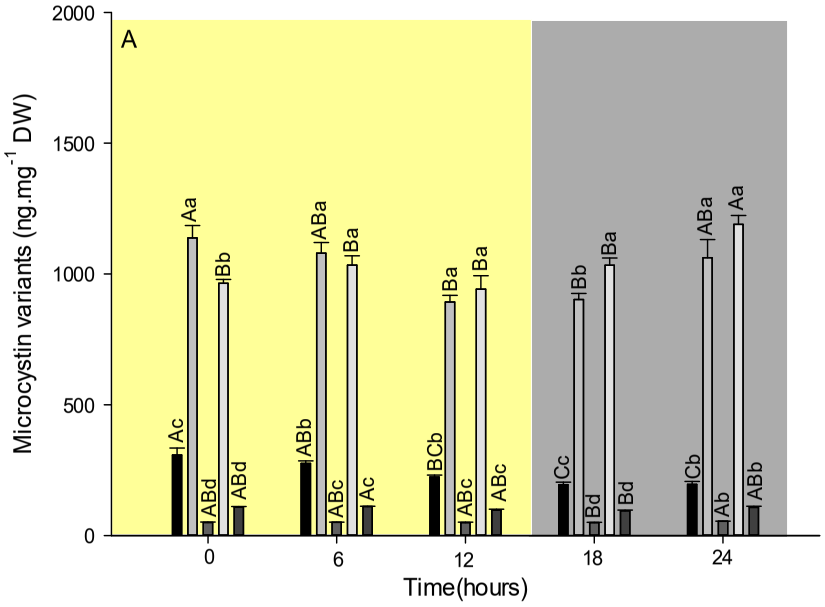

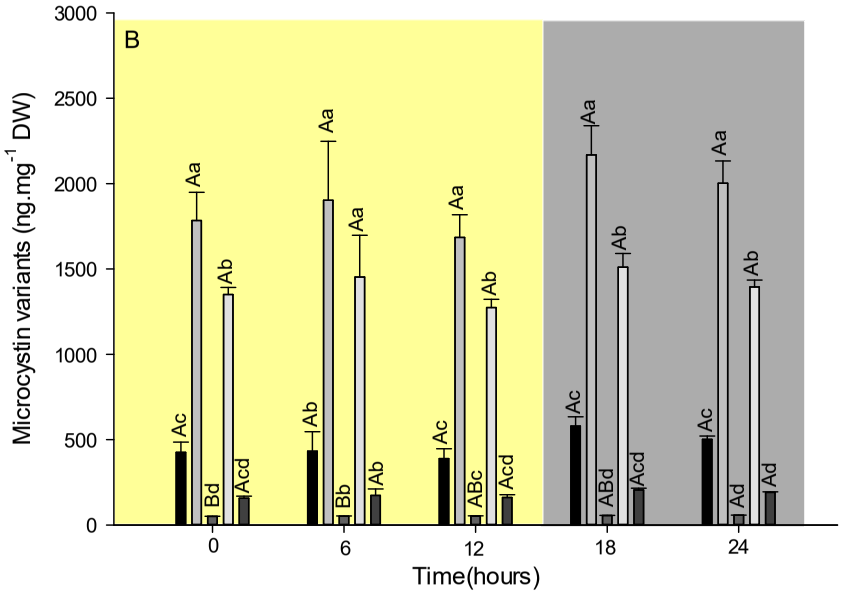

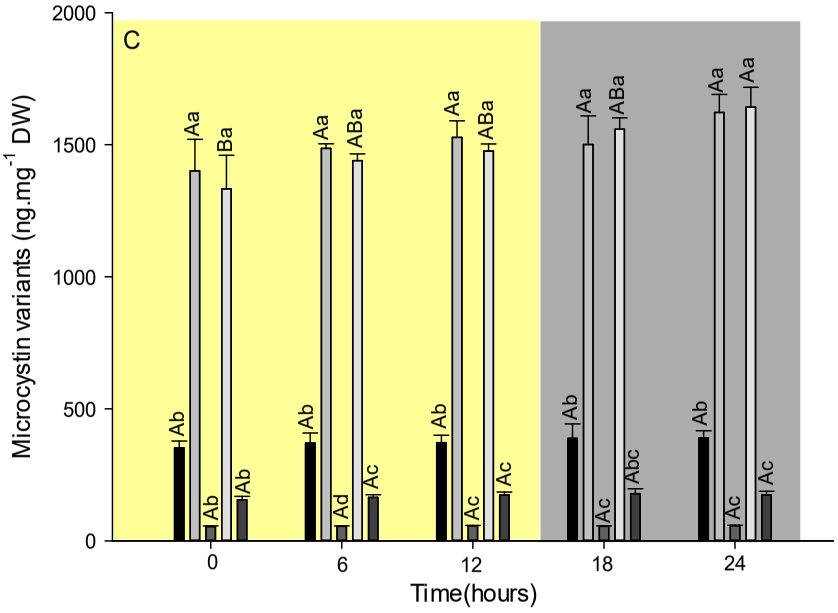
C
Microcystin variants (ng.mg-1 DW)
2000
1500
1000
500
0
Aa
Ba
Ab
Ab
Aa
ABa
Ad
Ac
Ab
Aa
ABa
Ac
Ac
Ab
Aa
ABa
Ac
Abc
Ab
Aa
Aa
Ac
Ac
0
6
12
18
24
Time(hours)

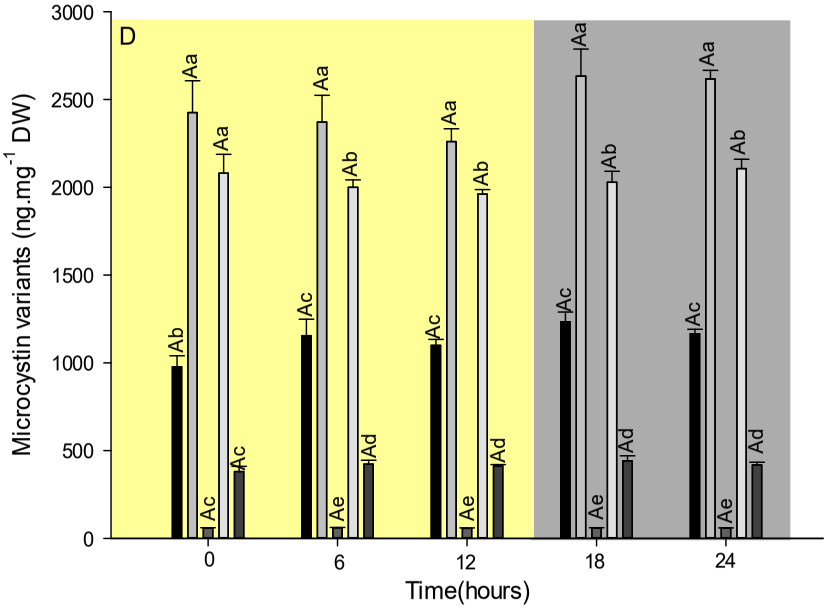
D
Microcystin variants (ng.mg-1 DW)
3000
2500
2000
1500
1000
500
0
Aa
Aa
Ab
Ac
Ac
Aa
Ab
Ae
Ad
Aa
Ab
Ae
Ad
Aa
Ab
Ae
Ad
Aa
Ab
Ae
Ad
0
6
12
18
24
Time(hours)

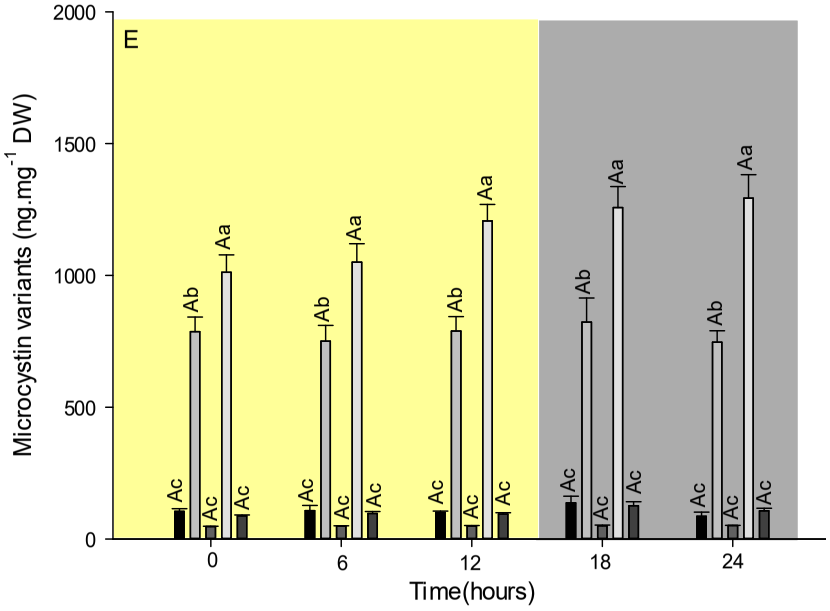
E
Microcystin variants (ng.mg-1 DW)
2000
1500
1000
500
0
Ac
Ab
Aa
Ac
0
6
12
18
24
Time(hours)

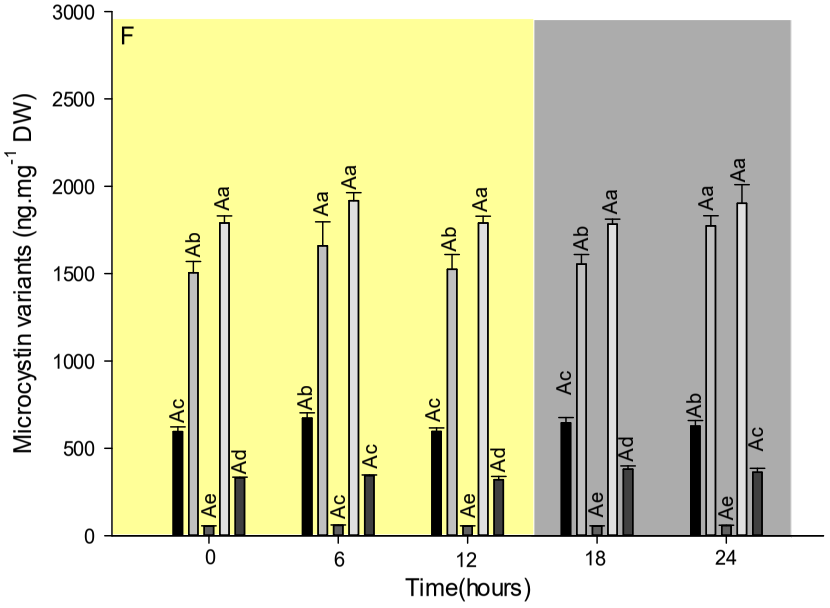
F
Microcystin variants (ng.mg-1 DW)
3000
2500
2000
1500
1000
500
0
Ac
Ab
Aa
Ae
Ad
0
6
12
18
24
Time(hours)

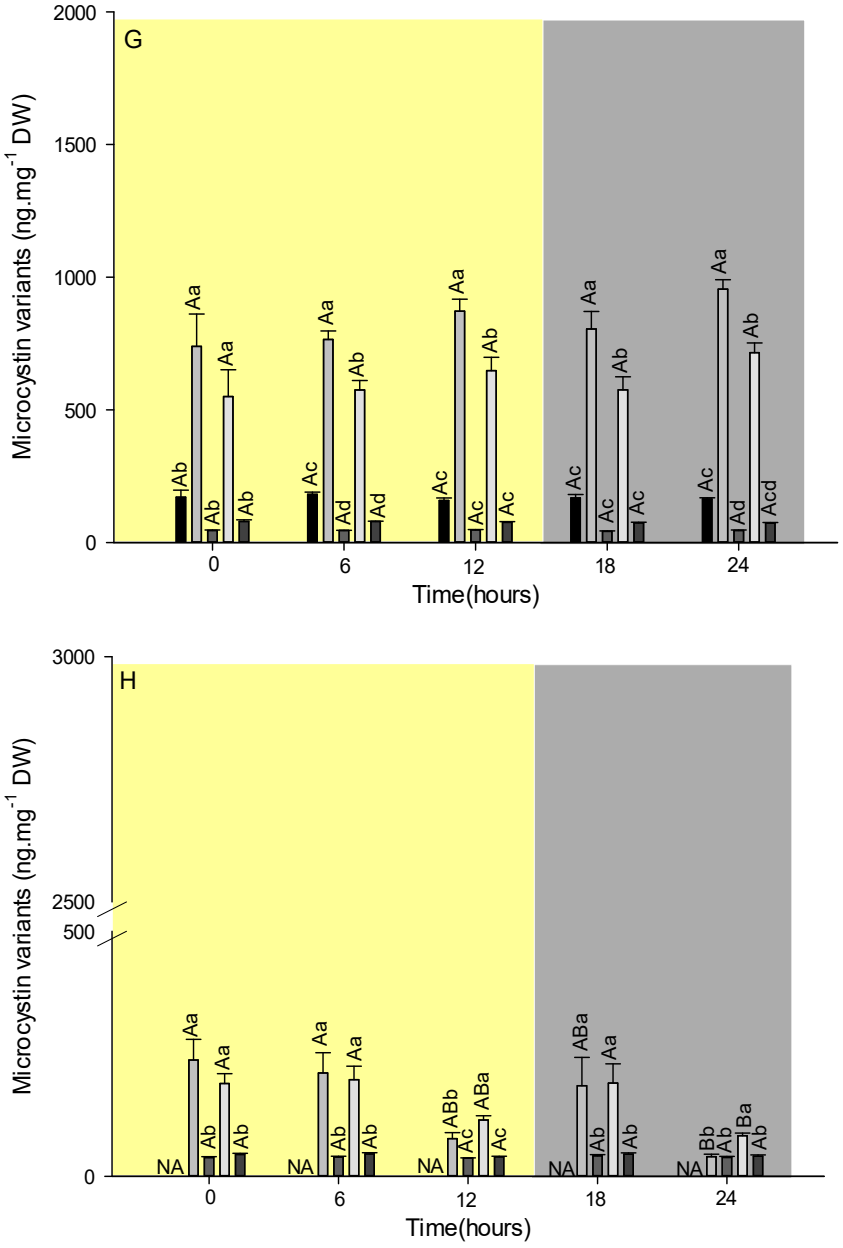

Figure 7. Production of different variants of microcystin in two growth phases. The microcystin content was collected at 6 hours' intervals during 24 hours and analyzed by LC-MS. **(A)** Control, Log phase; **(B)** Control, Stationary phase; **(C)** T1, Log phase; **(D)** T1, Stationary phase; **(E)** T2, Log phase; **(F)** T2, Stationary phase; **(G)** T3, Log phase; **(H)** T3, Stationary phase. Variants (*m*/*z*): 533 (black bars); 540 (light grey bars); 1023 (dark grey bars); 1037 (lighter grey bars); 1055 (darker grey bars). Values are presented as means ± error (n=4). Different letters represent average values that were judged to be statistically different ($P < 0.05$, Tukey test). Capital letters represent statistical differences between the hours at same variant, and lower-case letters demonstrate statistical differences between the variants at same hour.

In total, five MC's variants were detected as being produced by the strain CCM-UFV057 (Figure 7). The variants were named as 533, 540, 1023, 1037 and 1055, according to their respective *m*/*z* values. From them, the variants 540 and

1037 were always detected in greater amounts, regardless of treatment, or growth phase (Figure 7). Variant 1023 has a tendency to present the lowest values, considering all treatments and both log and stationary phases (Figure 7). Between the stationary and log phase there is an increase in the production of MCs between the control and both T1 and T2 (Figure 7A-B, 7C-D, 7E-F). However, T3 has a decrease in its production (Figure 7G-H). Variants do not exhibit a pattern of variation throughout the day (Figure 7). By comparing the treatments, T1 was the one that obtained the highest values of the variants, in the log and stationary phase (Figure 7C-D). The T3 was the one that displayed the smaller values, even leaving to produce one of the variants (533) in the stationary phase (Figure 15G-H).

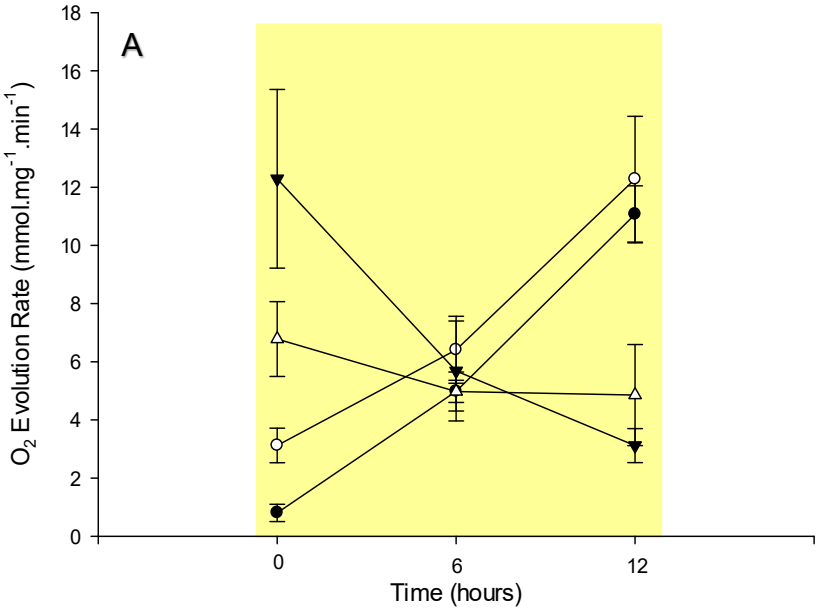

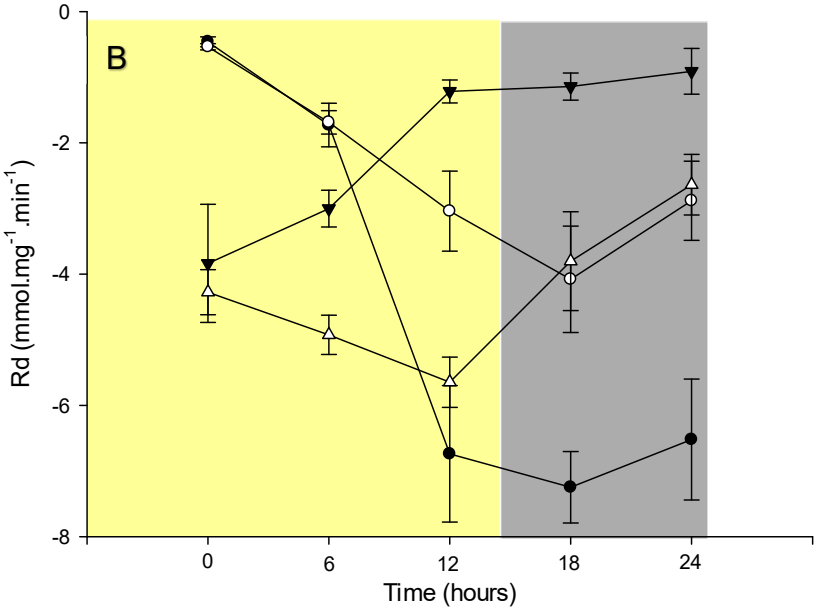

Figure 8. Photosynthesis and respiration rates in the log phase. The photosynthesis and respiration rates were measured using Clark`s electrode at 6 hours' intervals during 24 hours. **(A)** Photosynthesis; **(B)** Respiration. Treatments: Control (black circles): Standard BG-11_0 culture medium with 0.02 g·L^{-1} of sodium carbonate; T1 (white circles): BG-11_0 culture medium without any carbon source; T2 (black triangles): BG-11_0 culture medium with 0.016 g·L^{-1} of sodium bicarbonate; T3 (white triangles): BG-11_0 culture medium with 1.6 g·L^{-1} of sodium bicarbonate. Values are presented as means ± error (n=4). For statistical results, please see table S4 (log phase) and S5 (log phase) (Supplemental data).

Photosynthesis and respiration rates varied strongly among the treatments not only in the two growth phases, but also during the 24 hours of sampling. In the log phase, the photosynthesis of the control and of the treatment without exogenous addition of inorganic carbon (T1) showed a similar pattern, increasing throughout the day and reaching a maximum value at the end of the day (0-12h) (Figure 8A). By contrast, T3 did not lead to great variation in the photosynthetic rates throughout the day (Figure 8A). In an opposite way, T2 was characterized by a decreasing photosynthetic rate throughout the day, with its peak in the early morning (0h) (Figure 8A). This treatment (T2) also lead to a different respiratory behavior, compared to the other treatments. As consequence, the strain CCM-UFV057 had the highest respiratory rates during the light phase (0-6h), which exhibited a considerably decrease at the end of the day (12h), keeping it stable until the end of the night (18-24h) (Figure 8B). Moreover, control, T1 and T3 showed similar respiratory patterns: increased respiratory rates throughout the day (0-12h), with a gradual decrease at the end

of the day/early evening (12-18h) (Figure 8B). Despite the similar pattern, the control treatment displayed the highest respiratory rates at night (18-24h) (Figure

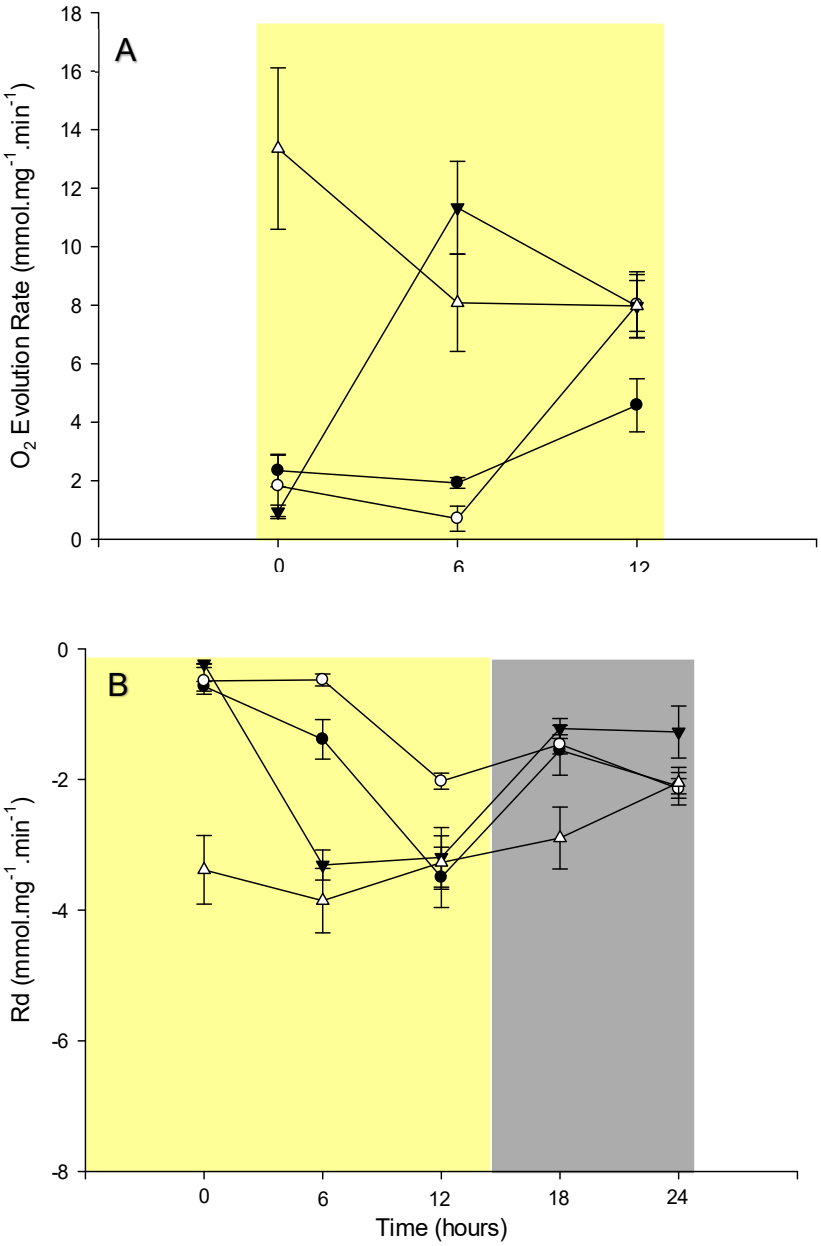

Figure 9. Photosynthesis and respiration rates in the stationary phase. The photosynthesis and respiration rates were measured using Clark`s electrode at 6 hours' intervals during 24 hours. (A) Photosynthesis; (B) Respiration. Treatments: Control (black circles): Standard BG-11$_0$ culture medium with 0.02 g·L^{-1} of sodium carbonate; T1 (white circles): BG-11$_0$ culture medium without any carbon source; T2 (black triangles): BG-11$_0$ culture medium with 0.016 g·L^{-1} of sodium bicarbonate; T3 (white triangles): BG-11$_0$ culture medium with 1.6 g·L^{-1} of sodium bicarbonate. Values are presented as means ± error (n=4). For statistical results, please see table S4 (stationary phase) and S5 (stationary phase) (Supplemental data).

Considering the stationary phase, no changes in photosynthetic rates along the day were observed with high inorganic carbon concentration (T3) (Figure 9A). It is important to mention that in the stationary phase, T3 lead to higher photosynthetic rates when compared to the other treatments, except at the end of the day, where all treatments displayed the same rate (Figure 9A). Control and T1 lead to similar patterns: low photosynthetic rates at the beginning of the day (0h), followed by gradual increasing until the end of the day (12h) (Figure 9A).

In the stationary phase, as observed in the log phase, T2 was characterized by an opposite pattern compared to the others treatments: starting with low photosynthetic rates, followed by a peak in the middle of the day (6h), with a later decreasing in the afternoon (12h) (Figure 9A). The respiratory rate performed by the strain CCM-UFV057 followed the same pattern considering control and T1: low rates in the early morning (0h), which increased during the day (6-12h), with a gradual decrease at night (18-24h) (Figure 9B). In the T3, the respiratory rates were high during the light phase (0-12h) and decreased over 24 hours, reaching the same level of all other treatments at the end of the night (24h) (Figure 9B).

4.3 Biochemical analysis

4.3.1 Chlorophyll *a*

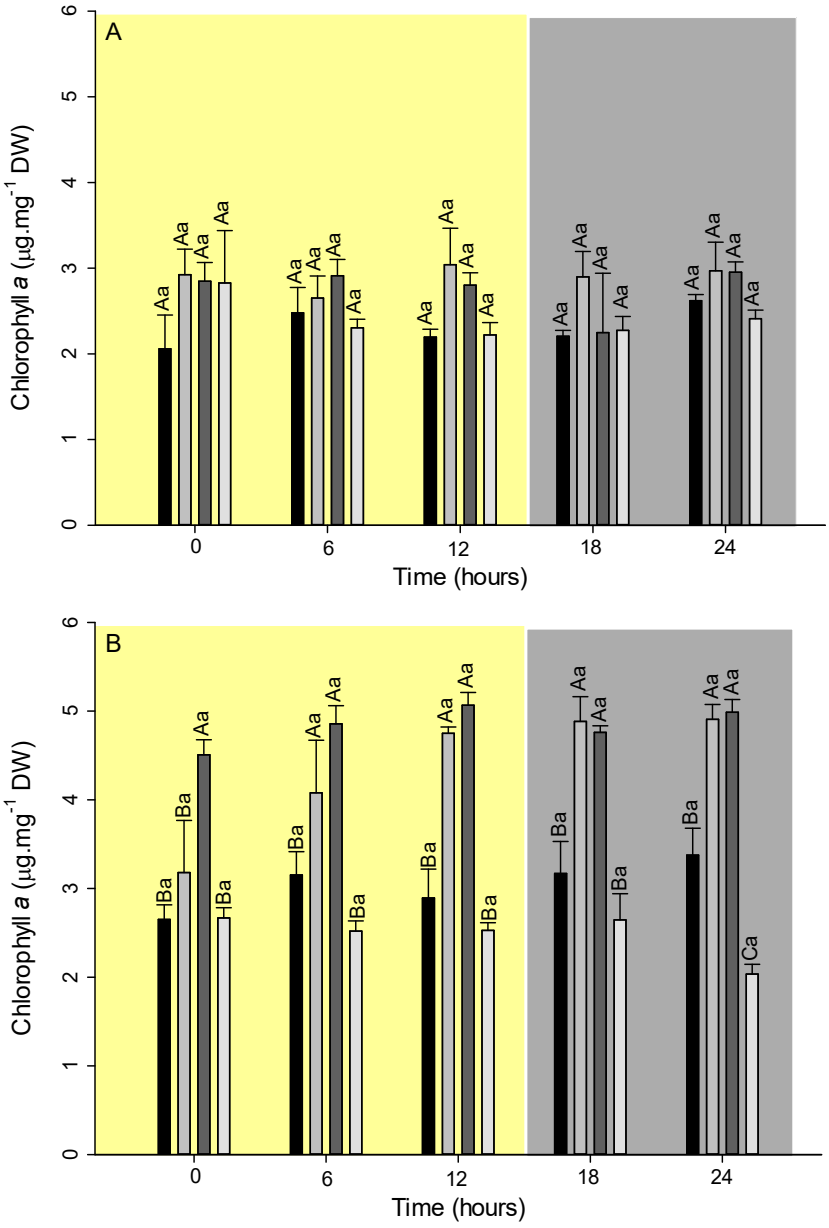

Figure 10. Variation in the chlorophyll *a* content in two growth phases. The chlorophyll *a* content was measured at 6 hours' intervals during 24 hours at OD_{653nm} and OD_{666nm}. **(A)** Log phase; **(B)** Stationary phase. Treatments: Control (black bars): BG-11_0 culture medium supplied with 0.02 g·L^{-1} of sodium carbonate; T1 (light grey bars): BG-11_0 culture medium without carbon source carbon; T2 (dark grey bars): BG-11_0 medium with 0.016 g·L^{-1} of sodium bicarbonate; T3 (lighter grey bars) $BG11_0$ medium with 1.6 g·L^{-1} of sodium bicarbonate. Values are presented as means ± error (n=4). Different letters represent average values that were judged to be statistically different (P < 0.05, Tukey test). Capital letters represent statistical differences between the treatments.

The chlorophyll *a* content did not change in the log phase, even considering both the treatments and along the time (Figure 10A). However, significant differences were observed in the stationary phase. The control and the T3 lead to the lowest values of chlorophyll *a* (Figure 10B), while the highest values were observed for the T1 and T2 (Figure 10B). Similar to that found in the log phase, there were no differences in the amount of chlorophyll *a* throughout the day for the same treatment.

4.3.2 Phycobiliproteins

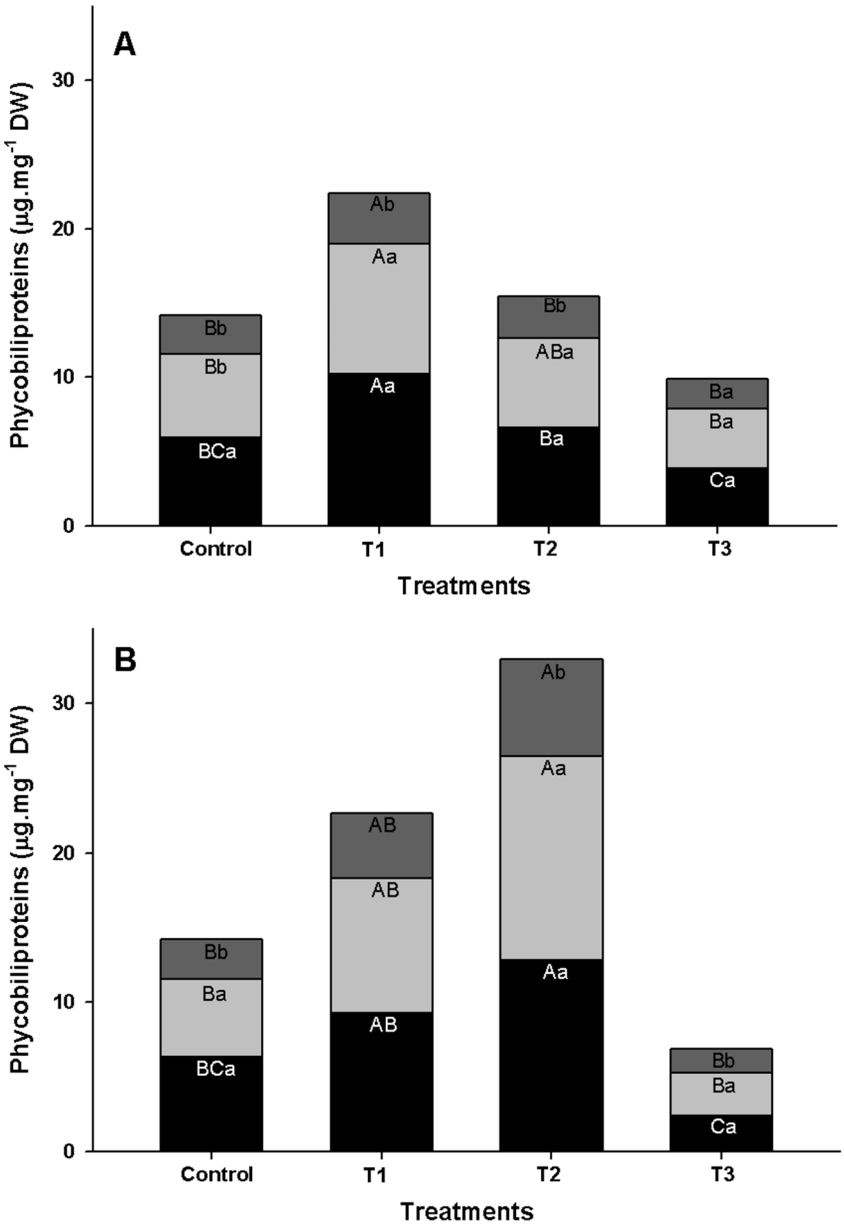

Figure 11. Variation in the phycobiliproteins content in two growth phases. The phycobiliproteins were measured in the middle of the light phase at OD_{565nm}, OD_{620nm} and OD_{650nm}. **(A)** Log phase; **(B)** Stationary phase. Phycobiliproteins: Phycocyanin (dark bars); Allophycocyanin (light grey bars); Phycoerythrin (dark grey bars). Values are presented as means ± error (n=4). Different letters represent average values that were judged to be statistically different ($P < 0.05$, Tukey test). Capital letters represent statistical differences between the treatments, and lower-case letters demonstrate statistical differences between the different phycobiliproteins in the same treatment.

The three pigments (phycobiliproteins – PBP) related to the cyanobacterial antenna complex (phycobilisomes), phycocyanin, allophycocyanin and phycoerythrin, were quantified in the middle of the light period of each growth phase. The strain CCM-UFV057 presents higher amounts of phycocyanin and allophycocyanin compared to those of phycoerythrin, in all treatments, regardless of the growth phase, log or stationary (Figure 11). However, it was observed that the amount of each pigment was different between treatments. Accordingly, in the log phase the treatment without carbon (T1) one of the large amounts of all three pigments was observed (Figure 11A). By contrast, the treatment with the highest inorganic carbon concentration (T3) yielded one of the lower phycobiliprotein content (Figure 11A). The T2 lead to the higher amounts of phycocyanin and allophycocyanin compared to the control (Figure 11A), however without statistical significance. Considering the time course, at the stationary phase, the T2 exhibited the highest pigment contents, for all treatments (Figure 11B), whereas the T3 had the lowest values in both phases (Figure 11B).

4.3.3 Total amino acids

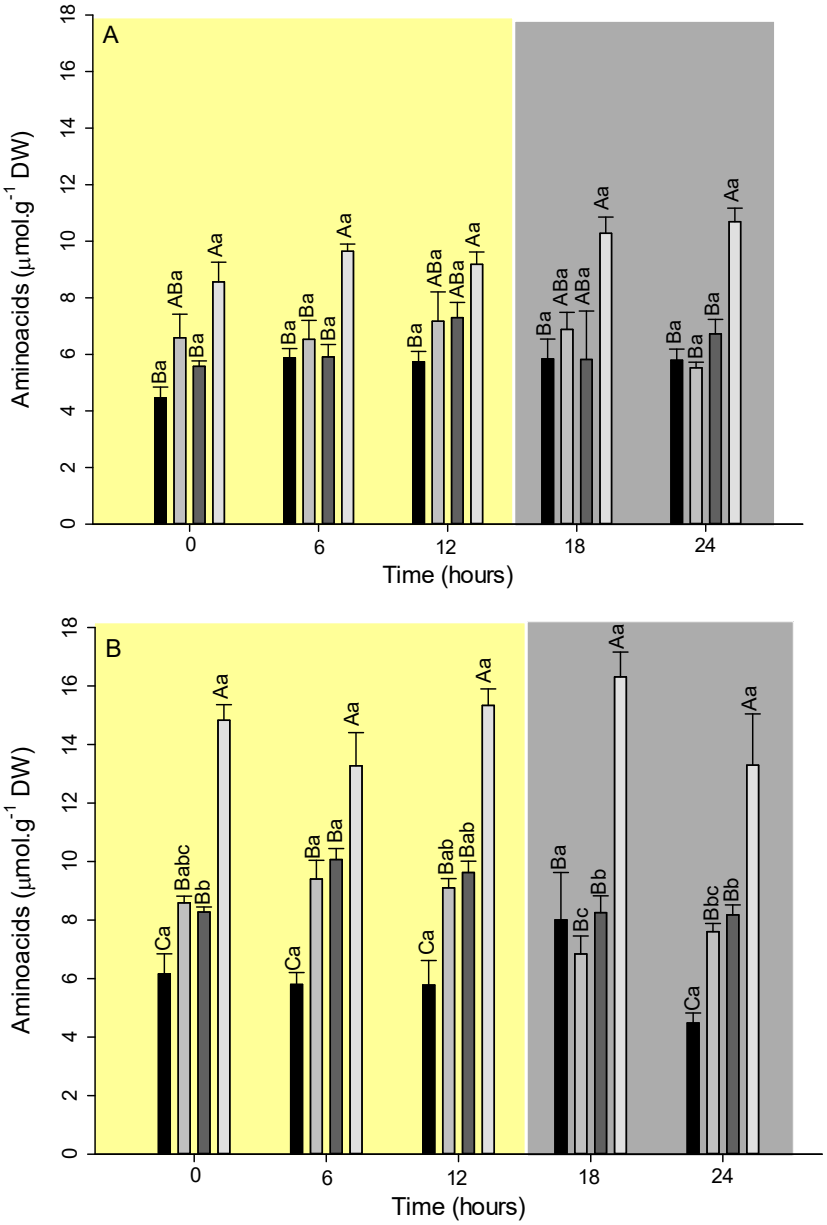

Figure 12. Variation in the amino acids content in two growth phases. The amino acids content was measured at 6 hours' intervals during 24 hours, at OD_{570nm}. **(A)** Log phase; **(B)** Stationary phase. Treatments: Control (black bars): BG-11_0 culture medium supplied with 0.02 g·L^{-1} of sodium carbonate; T1 (light grey bars): BG-11_0 culture medium without carbon source carbon; T2 (dark grey bars): BG-11_0 medium with 0.016 g·L^{-1} of sodium bicarbonate; T3 (lighter grey bars) $BG11_0$ medium with 1.6 g.L^{-1} of sodium bicarbonate. Values are presented as means ± error (n=4). Different letters represent average values that were judged to be statistically different (P < 0.05, Tukey test). Capital letters represent statistical differences between the treatments, and lower-case letters demonstrate statistical differences along time.

The total amino acid contents did not show significant variation considering a specific treatment, over 24 hours' interval, in both logarithmic and

stationary phases (Figure 12). The T3 (with the highest inorganic carbon concentration) lead to the higher amino acid contents among the treatments, in the two growth phases (Figure 12). The control and the other treatments displayed similar values of amino acids concentration in the log phase (Figure 12A). However, in the stationary phase the control (standard BG-11_0) yielded the lowest values (Figure 12B).

4.3.4 Total soluble proteins

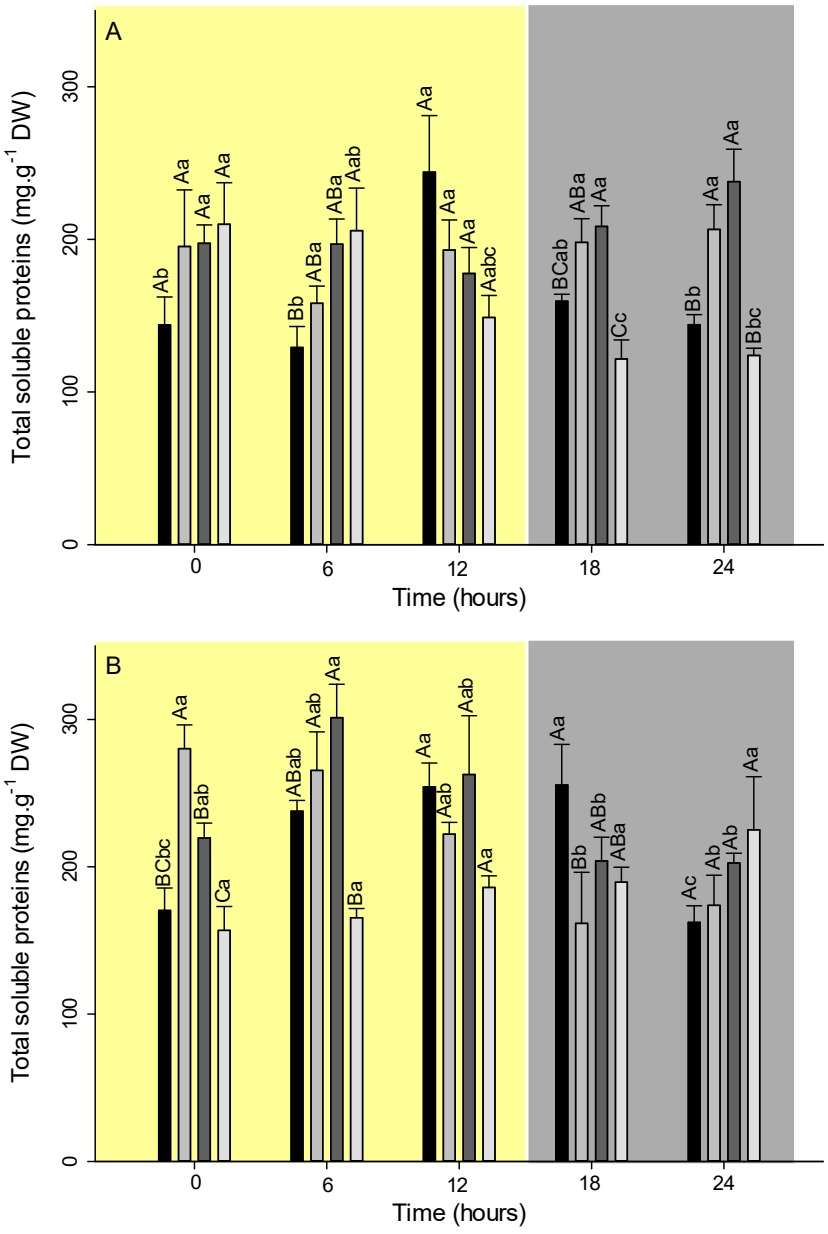

Figure 13. Variation in the total soluble proteins content in two growth phases. The proteins contents were measured at 6 hours' intervals during 24 hours, at OD_{595nm}. **(A)** Log phase; **(B)** Stationary phase. Treatments: Control (black bars): BG-11_0 culture medium supplied with 0.02

$g \cdot L^{-1}$ of sodium carbonate; T1 (light grey bars): $BG\text{-}11_0$ culture medium without carbon source carbon; T2 (dark grey bars): $BG\text{-}11_0$ medium with 0.016 $g \cdot L^{-1}$ of sodium bicarbonate; T3 (lighter grey bars) $BG11_0$ medium with 1.6 $g.L^{-1}$ of sodium bicarbonate. Values are presented as means ± error (n=4). Different letters represent average values that were judged to be statistically different ($P < 0.05$, Tukey test). Capital letters represent statistical differences between the treatments, and lower-case letters demonstrate statistical differences along time.

In the logarithmic phase, the T3 had high protein concentrations in the early hours of the day (0-6h), but a drop was observed in the late afternoon (12h); finally, this concentration was maintained until the end of the night (18-24h) (Figure 13A). Meanwhile, the control had low values at the beginning of the day (0-6h), a considerable peak in the late afternoon (12h), and again a drop in the amount of proteins (18h) and further maintenance (24h) (Figure 13A). The remaining treatments (T1 and T2) lead to relatively high protein concentrations during 24 hours' interval (Figure 13A). The most conspicuous differences among the treatments occurred at night (18-24h), with T1 and T2 having higher protein concentrations than control and T3 (Figure 13A).

In the stationary phase, during the day (0-6h), T1 and T2 remained with more proteins content than the other two treatments (Figure 13B). However, at night they fall (18h), and at the end of the night (24h) all treatments ended with similar values of proteins (Figure 13B). The control has an interesting variation, beginning with low concentrations (0h), increasing during the day, when reaches a maximum value in the end of the light phase (18h), and then return to the initials values in the end of the night (24h) (Figure 13B). The T3 has the lowest value between the treatments during the day (0-12h), and no variation along the 24h (Figure 13B).

4.3.5 Glycogen

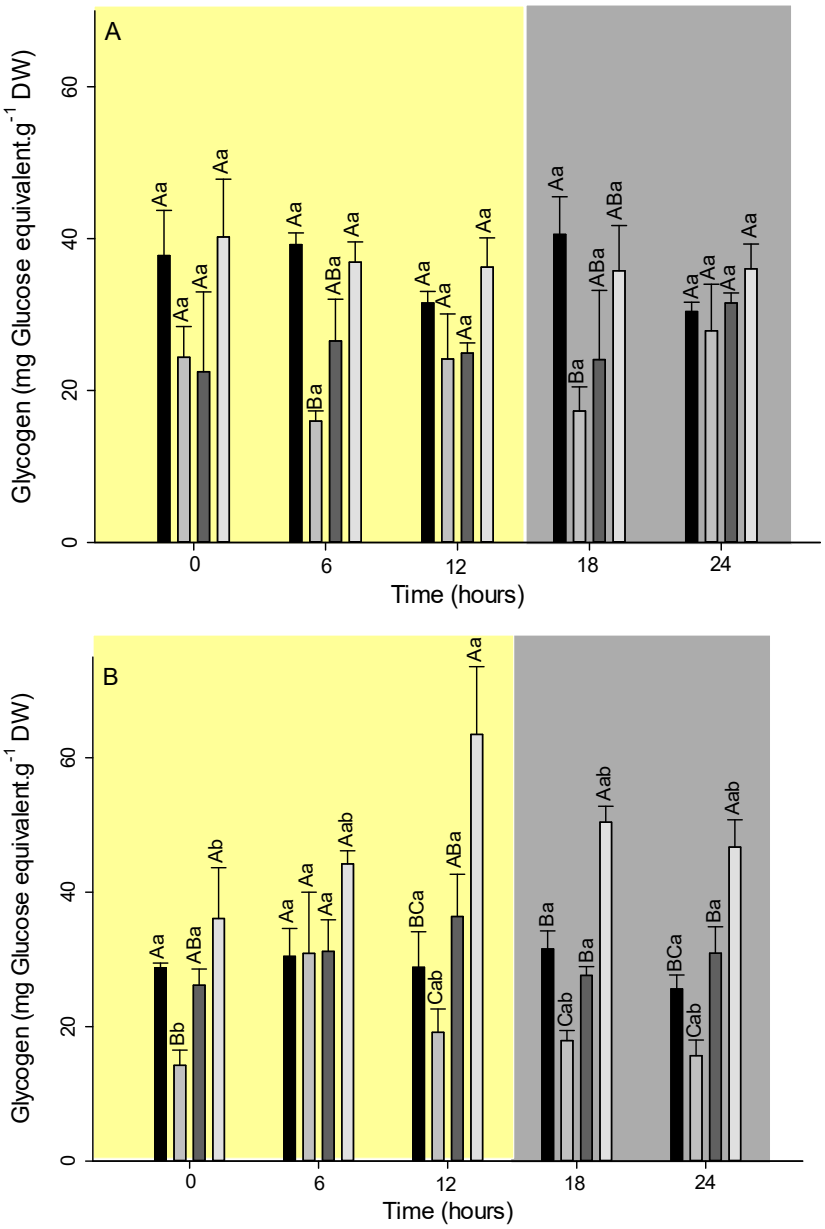

Figure 14. Variation in the glycogen content in two growth phases. The glycogen content was measured at 6 hours' intervals during 24 hours, as glucose equivalent, at OD_{340nm}. **(A)** Log phase; **(B)** Stationary phase. Treatments: Control (black bars): BG-11_0 culture medium supplied with 0.02 g·L^{-1} of sodium carbonate; T1 (light grey bars): BG-11_0 culture medium without carbon source carbon; T2 (dark grey bars): BG-11_0 medium with 0.016 g·L^{-1} of sodium bicarbonate; T3 (lighter grey bars) $BG11_0$ medium with 1.6 g.L^{-1} of sodium bicarbonate. Values are presented as means ± error (n=4). Different letters represent average values that were judged to be statistically different (P < 0.05, Tukey test). Capital letters represent statistical differences between the treatments, and lower-case letters demonstrate statistical differences along time.

Glycogen concentration did not display great variation throughout the day in the log phase (Figure 14A). However, T1 and T2 had a tendency to present

lower values, especially T1 (Figure 14A). In the stationary phase T3 was significantly higher than the other treatments during the 24 hours, with a peak at the end of the afternoon (12h) (Figure 14B). T1 had the lowest values (Figure 14B). Control and T2 obtained similar values throughout the day (Figure 14B).

5. DISCUSSION

Several attempts to correlate the production of MC to a specific function, or to several factors (Omidi et al., 2018) have been made. However, conflicting results in different studies, possibly due to the lack of standardized experimental designs, analysis using different culturing methods and growth conditions, have limited the definition of the role of MCs (Kardinaal et al., 2007; Neilan et al., 2013). Surprisingly, the effect of carbon concentrations conducted with *Microcystis* strains have shown similar results in studies conducted so far: at low concentrations of inorganic carbon the toxic species of *Microcystis* prevail under non-toxic ones (Jähnichen et al., 2007; Sandrini et al., 2016; Van De Waal et al., 2011; Yu et al., 2014; Zhang et al., 2012) .

To the best of our knowledge, this is the first study conducted with a filamentous heterocytous strain (CCM-UFV057). Perhaps more importantly, it demonstrates a clear influence of inorganic carbon concentration on the production of MCs (Figure 6). The absence of exogenous inorganic carbon source (T1) lead to the highest contents of microcystin, in both logarithmic and stationary phases (Figure 6). In contrast, the treatment with the highest inorganic carbon concentrations (T3) yielded the lowest MCs concentrations, which was even lower in the stationary phase (Figure 6). Our data corroborate with previous results (Jähnichen et al., 2007; Sandrini et al., 2016; Van De Waal et al., 2011; Yu et al., 2014), in studies conducted with the unicellular genus *Microcystis*, and is thus in good agreement with the first hypothesis of our work, that low carbon concentrations lead to an increase in the production of microcystin. Further studies are still required to fully elucidate whether this increased MC production is able to somehow modulate energetic production under low Ci concentration or it impacts the CCM in cyanobacteria.

It was also possible to observe that the carbon source, sodium carbonate or sodium bicarbonate, does not interfere in the total production of microcystin. Accordingly, both control and the T2, which were supplied with equimolar amounts of sodium carbonate and sodium bicarbonate, respectively, exhibited similar responses regarding microcystin production (Figure 6). It is important to highlight, however, that the most produced variants (540 and 1037) showed slight differences, considering their concentrations, between these two treatments (in the control the variant 540 present the highest values, and in the treatment T2, the variant 1037 was more abundant) (Figure 7). Taken together, it seems reasonable to suggest a differential role of these variants in the cyanobacterial metabolism. In this sense, the metabolites analyzed here showed different patterns between these treatments (Figures 10, 11, 12, 13 and 14), corroborating the motion of an exquisite metabolic adjustment. In agreement, variations in temperature (Dziallas and Grossart, 2011; Mowe et al., 2015) and in the amino acids supply (Dai et al., 2019; Van De Waal et al., 2011) have been shown to modify the proportion of different MCs variants. These results, coupled with a specific function on overall cyanobacterial metabolism, may be of relevance for short term response to stress conditions. Further studies are required to fully explore this intriguing connection.

Taking into consideration the physiological responses of the strain CCM-UFV to the fluctuations in the Ci levels, it seems reasonable to anticipate that our results are highly relevant and can help to enhance our understanding on the microcystin role on cyanobacterial metabolism. In T1, in which the inorganic carbon supply was absent, the strain CCM-UFV057 showed one of the highest amounts of chlorophyll *a* (4.9 µg chl*a* mg^{-1} DW) (Figure 10). It is known that higher chlorophyll concentrations are directed related to the reaction centers efficiency (Burnap et al., 2015). Additionally, according to the same authors, higher reaction centers efficiency leads to higher photosynthetic electron transport (PSET), which in turn drives to an increasing growth rate. These assumptions are in good agreement with our own results regarding the generation time, which was lower for the treatment T1 (63.41 hours) (Table 1). Furthermore, the results from

photosynthesis and respiration (Figures 8 and 9) showed that the T1 was characterized by the higher photosynthetic efficiency of the strain CCM-UFV057, as can be inferred by the high growth rates (Table 1), even though it did not perform the highest photosynthetic rates (Figures 8A and 9A) coupled with one of the lowest respiratory rates (Figures 8B and 9B), meaning a high energetic efficiency in terms of carbon uptake/assimilation.

This high efficiency in carbon assimilation can also be explained, at least partially, by the high levels of proteins (Figure 13) as well as the low concentrations of amino acids (Figure 12) and glycogen (Figure 14). In this case, it is plausible to suggest that most of the fixed carbon is likely being used for structural synthesis (high protein contents) followed by low amino acids and glycogen contents. Accordingly, the glycogen synthesis is related to carbon storage, removing its excess (Burnap et al., 2015), which is not the case, since there is no inorganic carbon supply in this treatment. Additionally, given the high protein contents, it seems that the fixed carbon skeletons are being directed towards the formation of amino acids and later converted to proteins (Burnap et al., 2015; Huege et al., 2011; Schwarz et al., 2013). It is important to mention that the CCM-UFV057 is a nitrogen-fixing strain and was cultivated without any inorganic nitrogen source (BG-11_0). As consequence, higher photosynthetic rates are required for sustaining the BNF, which requires high amounts of both, reduced cofactors and ATP (Zhang et al., 2018).

It is interesting to note that the T2 showed for metabolites such as chlorophyll *a* and phycobiliproteins, which are directly related with light collecting, similar values to those found for T1 (Figures 10 and 11). However, the T1 (12.5 $\mu mol \cdot L^{-1}$ of inorganic carbon from air diffusion), as described above lead to a higher photosynthetic efficiency, which means that even without carbon supplementation, the strain CCM-UFV057 produced the same amount of pigments amounts that the T2 (supplied with 188 $\mu mol \cdot L^{-1}$ of inorganic carbon) indicating a metabolic adjustment that is most likely able to support high photosynthetic rates. Collectively, our results provide compelling evidence into the physiological adaptations explaining the remarkable ability of microcystin-

producers strains to cope with changes in inorganic carbon levels mediated by complex metabolic reprograming. Although we could not experimentally elucidate this feature, further studies including the full genome sequencing of this strain and a metabolite profile are clearly required to fully elucidate the important of this mechanism.

Interestingly, the T3, in which higher carbon supplementation was applied and that showed the highest pH values (Supplemental Figure 2) over the cultivation, did not culminate with changes in growth of CCM-UFV057 compared to the other treatments (Figure 3). This results corroborate those found by Touloupakis et al. (2016), that shown that a pH range of 7 to 10 in the strain *Synechocystis* sp. PCC6803 did not affect its growth. Moreover, studies conducted by Dwivedi et al. (1994) using a *Microcystis aeruginosa* and a *Hapalosiphon welwitschii* demonstrated that the internal pH had negligible changes when they were submitted to a range of different values of pHs, 7 to 10 (Touloupakis et al., 2016; Dwivedi et al., 1994). Taken together, these results indicate that despite in pH values the high carbon supplementation did not compromise the cyanobacterial growth. This corroborates with other studies that demonstrate that, even in atmospheric ambient conditions, cyanobacterial RubisCO already face saturating carbon concentrations (Badger et al., 2006). In addition, high carbon concentrations increases the absorption of Ci, however, as the rate of assimilation remains the same, there is most likely a greater “leak” of carbon into the medium (Burnap et al., 2015; Tchernov et al., 2003). Yet, this high carbon loss occurs, it seems plausible that the high carbon concentration decreases the energy expended by the cell, since there is a lower induction of CCM, which is a high cost process (Burnap et al., 2015). Under high Ci, most of the newly fixed carbon is leaving the Calvin-Benson cycle in the direction of the carbohydrate metabolism and storage (Huege et al., 2011; Schwarz et al., 2013), which is consistent with the results found here for the strain CCM-UFV057 in the T3 (Figure 14). Moreover, the glycogen pool seems to play an essential role in buffering cellular metabolism against unbalanced C/N availability (Burnap et al., 2015). Moreover, by using mutant strains for glycogen synthesis it was

demonstrated that pyruvate and 2-oxoglutarate (2-OG) are released into the medium under nitrogen limitation conditions (Carrieri et al., 2012; Xu et al., 2013). Since CCM-UFV057 has the ability to fix atmospheric nitrogen, it is highly unlikely that this limitation is occurring. Future studies are clearly required to identify exactly where this C and N pool is directed and to dissect how and to what extent microcystin co-ordinate the flux through the central metabolism.

Collectively, growth and physiology data indicated that the T3 lead to a typical responses of strains subjected to high carbon concentrations and that the strain CCM-UFV057 did not appear to be suffering from any type of stress derived from high pH values. Moreover, the very low production of microcystin does not appear to interfere with the growth and development of this strains under this condition. On the other hand, the T1 has similar physiology to the treatment T2 (carbon concentrations equal to the control), having significant differences in the amount of microcystin, which leads us to conclude that microcystin may play an important role in carbon metabolism, as previously suggested by Meissner et al. (2014) and Zilliges et al. (2011).

It has been also demonstrated that more than two-thirds of MCs are physically attached to the thylakoids membranes (Lefebvre et al., 2005; Shi et al., 1995; Young et al., 2008). Nevertheless, it has been also revealed that MCs are generally localized within carboxysomes following immunogold labeling (Gerbersdorf, 2006). It has also been shown that microcystin binds to the major subunit of RubisCO (Zilliges et al., 2011). In addition, a study conducted by Meissner et al. (2014) with high-light-stressed cells of *M. aeruginosa*, showed that these cells have an increased accumulation of photorespiratory intermediates such as glycolate. On the other hand, its mutant showed decreased levels of glycolate (Meissner et al., 2014). These results suggested that microcystin play a key role in the partitioning of carbon from CBB to photorespiration (Burnap et al., 2015). Taken together, these data and other studies implies that microcystin-binding is somehow influencing RubisCO specificity or activity, but further studies, including RubisCO expression, protein

levels and enzymatic activity, are clearly required to fully clarify the role of this toxin.

6. CONCLUNDING REMARKS

Due to the high toxicity of microcystin (MCs) for eukaryotes, the vast majority of the researches is usually focused on the harmful effects of MCs on humans, animals, and aquatic organisms. However, their natural physiological and/or ecological functions on cyanobacteria remain rather unclear (Merel et al., 2013a, 2013b). Over the years, several independent studies have been performed to clarify questions such as why cyanobacteria produce this toxin, after all, MCs are N-rich and high cost products. As consequence, since MCs-producers pay a high energetic price for MC synthesis, they could be an effective factor in the cellular metabolism beyond their toxicity (Omidi et al., 2018). Ours results suggested that, despite significant changes in MC production in response to Ci levels coupled with changes in photosynthesis and respiration, the growth rate, based on optical density, had minor changes between the treatments (Figure 3).This indicates that the high energetic cost required for the synthesis of MC is, most likely, associated with an increased in the energetic production, and the probably action of MC in the specificity or activity of RubisCO.

7. REFERENCES

Altermann, W., Kazmierczak, J., 2003. Archean microfossils: a reappraisal of early life on Earth. Res. Microbiol. 154, 611–617. https://doi.org/https://doi.org/10.1016/j.resmic.2003.08.006

Badger, M.R., Price, G.D., Long, B.M., Woodger, F.J., 2006. The environmental plasticity and ecological genomics of the cyanobacterial CO2 concentrating mechanism. J. Exp. Bot. 57, 249–265.

Bishop, C.T., Anet, E.F.L.J., Gorham, P.R., 1959. Isolation and Identification of the Fast-Death Factor in Microcystis Aeruginosa Nrc-1. Can. J. Biochem. Physiol. 37, 453–471. https://doi.org/10.1139/o59-047

Botes, D.P., Tuinman, A.A., Wessels, P.L., Viljoen, C.C., Kruger, H., Williams, D.H., Santikarn, S., Smith, R.J., Hammond, S.J., 1984. The structure of

cyanoginosin-LA, a cyclic heptapeptide toxin from the cyanobacterium Microcystis aeruginosa. J. Chem. Soc. Perkin Trans. 1 2311–2318. https://doi.org/10.1039/P19840002311

Bradford, M.M., 1976. A rapid and sensitive method for the quantitation of microgram quantities of protein utilizing the principle of protein-dye binding. Anal. Biochem. 72, 248–254. https://doi.org/https://doi.org/10.1016/0003-2697(76)90527-3

Briand, E., Bormans, M., Gugger, M., Dorrestein, P.C., Gerwick, W.H., 2016. Changes in secondary metabolic profiles of Microcystis aeruginosa strains in response to intraspecific interactions. Environ. Microbiol. 18, 384–400. https://doi.org/10.1111/1462-2920.12904

Briand, E., Escoffier, N., Straub, C., Sabart, M., Quiblier, C., Humbert, J.-F., 2008. Spatiotemporal changes in the genetic diversity of a bloom-forming Microcystis aeruginosa (cyanobacteria) population. Isme J. 3, 419.

Burnap, R., Hagemann, M., Kaplan, A., 2015. Regulation of CO2 Concentrating Mechanism in Cyanobacteria. Life 5, 348–371. https://doi.org/10.3390/life5010348

Carmichael, W.W., 2001. Health Effects of Toxin-Producing Cyanobacteria: “The CyanoHABs.” Hum. Ecol. Risk Assess. An Int. J. 7, 1393–1407. https://doi.org/10.1080/20018091095087

Carmichael, W.W., Gorham, P.R., 1981. The Mosaic Nature of Toxic Blooms of Cyanobacteria BT - The Water Environment: Algal Toxins and Health, in: Carmichael, W.W. (Ed.), . Springer US, Boston, MA, pp. 161–172. https://doi.org/10.1007/978-1-4613-3267-1_12

Carrieri, D., Paddock, T., Maness, P.-C., Seibert, M., Yu, J., 2012. Photo-catalytic conversion of carbon dioxide to organic acids by a recombinant cyanobacterium incapable of glycogen storage. Energy Environ. Sci. 5, 9457. https://doi.org/10.1039/c2ee23181f

Castenholz, R., 2001. Phylum BX. Cyanobacteria Oxigenic Photosynthetic Bacteria, in: Bergey’s Manual of Systematic Bacteriology. Springer New York, New York, NY, pp. 473–599. https://doi.org/10.1007/978-0-387-21609-

6_27

Christiansen, G., Fastner, J., Erhard, M., Börner, T., Dittmann, E., 2003. Microcystin biosynthesis in Planktothrix: Genes, evolution, and manipulation. J. Bacteriol. 185, 564–572. https://doi.org/10.1128/JB.185.2.564-572.2003

Codd, G.A., Morrison, L.F., Metcalf, J.S., 2005. Cyanobacterial toxins: Risk management for health protection. Toxicol. Appl. Pharmacol., 203:264–272. doi: 10.1016/j.taap.2004.02.016.

Cross, J.M., von Korff, M., Altmann, T., Bartzetko, L., Sulpice, R., Gibon, Y., Palacios, N., Stitt, M., 2006. Variation of Enzyme Activities and Metabolite Levels in 24 Arabidopsis Accessions Growing in Carbon-Limited Conditions. Plant Physiol. 142, 1574–1588. https://doi.org/10.1104/pp.106.086629

Dai, R., Zhou, Y., Chen, Y., Zhang, X., Yan, Y., An, D., 2019. Effects of arginine on the growth and microcystin-LR production of Microcystis aeruginosa in culture. Sci. Total Environ. 651, 706–712. https://doi.org/https://doi.org/10.1016/j.scitotenv.2018.09.213

Davis, T.W., Berry, D.L., Boyer, G.L., Gobler, C.J., 2009. The effects of temperature and nutrients on the growth and dynamics of toxic and non-toxic strains of Microcystis during cyanobacteria blooms. Harmful Algae 8, 715–725. https://doi.org/https://doi.org/10.1016/j.hal.2009.02.004

de Figueiredo, D.R., Azeiteiro, U.M., Esteves, S.M., Gonçalves, F.J.M., Pereira, M.J., 2004. Microcystin-producing blooms—a serious global public health issue. Ecotoxicol. Environ. Saf. 59, 151–163. https://doi.org/https://doi.org/10.1016/j.ecoenv.2004.04.006

de Marsac, N.T., Houmard, J., 1988. Complementary Chromatic Adaptation: Physiological Conditions and Action Spectra, in: Methods in Enzymology. Elsevier, pp. 318–328. https://doi.org/10.1016/0076-6879(88)67037-6

Dittmann, E., Börner, T., 2005. Genetic contributions to the risk assessment of microcystin in the environment. Toxicol. Appl. Pharmacol. 203, 192–200. https://doi.org/https://doi.org/10.1016/j.taap.2004.06.008

Dittmann, E., Meißner, K., Börner, T., 1996. Conserved sequences of peptide synthetase genes in the cyanobacterium Microcystis aeruginosa. Phycologia

35, 62–67. https://doi.org/10.2216/i0031-8884-35-6s-62.1

Dittmann, E., Neilan, B.A., Erhard, M., Von Döhren, H., Börner, T., 1997. Insertional mutagenesis of a peptide synthetase gene that is responsible for hepatotoxin production in the cyanobacterium Microcystis aeruginosa PCC 7806 . Mol. Microbiol. 26, 779–787. https://doi.org/10.1046/j.1365-2958.1997.6131982.x

Dong, X., Zeng, S.,Bai, F., Li, D., He, M., 2016. Extracellular microcystin prediction based on toxigenic Microcystis detection in a eutrophic lake. Scientific Reports volume6, Article number: 20886.

Dwivedi, A., Srinivas, U.K., Singh, H.N., Kumar, H.D., 1994. Regulatory effect of external pH on the intracellular pH in alkalophilic cyanobacteria Microcystis aeruginosa and Hapalosiphon welwitschii. J. Gen. Appl. Microbiol., 40, 261-263.

Dziallas, C., Grossart, H.-P., 2011. Increasing Oxygen Radicals and Water Temperature Select for Toxic Microcystis sp. PLoS One 6, e25569.

Fernie, A.R., Roscher, A., Ratcliffe, R.G., Kruger, N.J., 2001. Fructose 2,6-bisphosphate activates pyrophosphate: fructose-6-phosphate 1-phosphotransferase and increases triose phosphate to hexose phosphate cycling in heterotrophic cells. Planta 212, 250–263. https://doi.org/10.1007/s004250000386

Fewer, D.P., Rouhiainen, L., Jokela, J., Wahlsten, M., Laakso, K., Wang, H., Sivonen, K., 2007. Recurrent adenylation domain replacement in the microcystin synthetase gene cluster. BMC Evol. Biol. 7, 183. https://doi.org/10.1186/1471-2148-7-183

Fewer, D.P., Wahlsten, M., Österholm, J., Jokela, J., Rouhiainen, L., Kaasalainen, U., Rikkinen, J., Sivonen, K., 2013. The Genetic Basis for O-Acetylation of the Microcystin Toxin in Cyanobacteria. Chem. Biol. 20, 861–869. https://doi.org/https://doi.org/10.1016/j.chembiol.2013.04.020

Finking, R., Marahiel, M.A., 2004. Biosynthesis of Nonribosomal Peptides. Annu. Rev. Microbiol. 58, 453–488. https://doi.org/10.1146/annurev.micro.58.030603.123615

Flores, E., Herrero, A., 2009. Compartmentalized function through cell differentiation in filamentous cyanobacteria. Nat. Rev. Microbiol. 8, 39.

Gao, X., Liu, K., Qiu, B.S., 2011. An investigation on the genetic background of Nostoc flagelliforme by similarity analysis of its partial genomic DNA and phylogenetic comparison of deduced related species. Acta Physiol. Plant. 33, 1301–1318. https://doi.org/10.1007/s11738-010-0662-z

Geada, P., Pereira, R.N., Vasconcelos, V., Vicente, A.A., Fernandes, B.D., 2017. Assessment of synergistic interactions between environmental factors on Microcystis aeruginosa growth and microcystin production. Algal Res. 27, 235–243. https://doi.org/10.1016/j.algal.2017.09.006

Genuário, D.B., Corrêa, D.M., Komárek, J., Fiore, M.F., 2013. Characterization of freshwater benthic biofilm-forming Hydrocoryne (Cyanobacteria) isolates from Antarctica. J. Phycol. 49, 1142–1153. https://doi.org/10.1111/jpy.12124

Genuário, D.B., Vaz, M.G.M.V., Santos, S.N., Kavamura, V.N., Melo, I.S., 2019. Cyanobacteria From Brazilian Extreme Environments. Microb. Divers. Genomic Era 265–284. https://doi.org/10.1016/B978-0-12-814849-5.00016-2

Gerbersdorf, S.U., 2006. An advanced technique for immuno-labelling of microcystins in cryosectioned cells of Microcystis aeruginosa PCC 7806 (cyanobacteria): Implementations of an experiment with varying light scenarios and culture densities. Toxicon 47, 218–228. https://doi.org/https://doi.org/10.1016/j.toxicon.2005.10.019

Giovannoni, S.J., Turner, S., Olsen, G.J., Barns, S., Lane, D.J., Pace, N.R., 1988. Evolutionary relationships among cyanobacteria and green chloroplasts. J. Bacteriol. 170, 3584–3592. https://doi.org/10.1128/jb.170.8.3584-3592.1988

Hagenbuch, B., Gui, C., 2008. Xenobiotic transporters of the human organic anion transporting polypeptides (OATP) family. Xenobiotica 38, 778–801. https://doi.org/10.1080/00498250801986951

Huege, J., Goetze, J., Schwarz, D., Bauwe, H., Hagemann, M., Kopka, J., 2011. Modulation of the Major Paths of Carbon in Photorespiratory Mutants of Synechocystis. PLoS One 6, e16278.

Jähnichen, S., Ihle, T., Petzoldt, T., Benndorf, J., 2007. Impact of Inorganic Carbon Availability on Microcystin Production by Microcystis aeruginosa PCC 7806. Appl. Environ. Microbiol. 73, 6994 LP – 7002. https://doi.org/10.1128/AEM.01253-07

Jähnichen, S., Petzoldt, T., Benndorf, J., 2001. Evidence for control of microcystin dynamics in Bautzen Reservoir (Germany) by cyanobacterial population growth rates and dissolved inorganic carbon. Fundam. Appl. Limnol. 150, 177–196. https://doi.org/10.1127/archiv-hydrobiol/150/2001/177

Jährlichen, S., Ihle, T., Petzoldt, T., Benndorf, J., 2007. Impact of inorganic carbon availability on microcystin production by Microcystis aeruginosa PCC 7806. Appl. Environ. Microbiol. 73, 6994–7002. https://doi.org/10.1128/AEM.01253-07

Jang, M.-H., Ha, K., Joo, G.-J., Takamura, N., 2003. Toxin production of cyanobacteria is increased by exposure to zooplankton. Freshw. Biol. 48, 1540–1550. https://doi.org/10.1046/j.1365-2427.2003.01107.x

Kalliokoski, A., Niemi, M., 2009. Impact of OATP transporters on pharmacokinetics. Br. J. Pharmacol. 158, 693–705. https://doi.org/10.1111/j.1476-5381.2009.00430.x

Kardinaal, W.E.A., Tonk, L., Janse, I., Hol, S., Slot, P., Huisman, J., Visser, P.M., 2007. Competition for Light between Toxic and Nontoxic Strains of the Harmful Cyanobacterium Microcystis Appl. Environ. Microbiol. 73, 2939 LP – 2946. https://doi.org/10.1128/AEM.02892-06

Knoll, A.H., 2008. Cyanobacteria and Earth history. cyanobacteria Mol. Biol. genomics, Evol. 495.

Krishnamurthy, T., Carmichael, W.W., Sarver, E.W., 1986. Toxic peptides from freshwater cyanobacteria (blue-green algae). I. Isolation, purification and characterization of peptides from Microcystis aeruginosa and Anabaena flos-aquae. Toxicon 24, 865–873. https://doi.org/https://doi.org/10.1016/0041-0101(86)90087-5

LeBlanc Renaud, S., Pick, F.R., Fortin, N., 2011. Effect of Light Intensity on the

Relative Dominance of Toxigenic and Nontoxigenic Strains of Microcystis aeruginosa Appl. Environ. Microbiol. 77, 7016 LP – 7022.

Lefebvre, S., Lawson, T., Fryer, M., Zakhleniuk, O. V, Lloyd, J.C., Raines, C.A., 2005. Increased Sedoheptulose-1,7-Bisphosphatase Activity in Transgenic Tobacco Plants Stimulates Photosynthesis and Growth from an Early Stage in Development. Plant Physiol. 138, 451 LP – 460. https://doi.org/10.1104/pp.104.055046

Lürling, M., van Oosterhout, F., Faassen, E., 2017 Eutrophication and Warming Boost Cyanobacterial Biomass and Microcystins. Toxins (Basel). 2017;9(2):64. doi:10.3390/toxins9020064

Meissner, S., Steinhauser, D., Dittmann, E., 2014. Metabolomic analysis indicates a pivotal role of the hepatotoxin microcystin in high light adaptation of Microcystis. Environ. Microbiol. 17, 1497–1509. https://doi.org/10.1111/1462-2920.12565

Merel, S., Villarín, M.C., Chung, K., Snyder, S., 2013a. Spatial and thematic distribution of research on cyanotoxins. Toxicon 76, 118–131. https://doi.org/https://doi.org/10.1016/j.toxicon.2013.09.008

Merel, S., Walker, D., Chicana, R., Snyder, S., Baurès, E., Thomas, O., 2013b. State of knowledge and concerns on cyanobacterial blooms and cyanotoxins. Environ. Int. 59, 303–327. https://doi.org/https://doi.org/10.1016/j.envint.2013.06.013

Mowe, M.A.D., Porojan, C., Abbas, F., Mitrovic, S.M., Lim, R.P., Furey, A., Yeo, D.C.J., 2015. Rising temperatures may increase growth rates and microcystin production in tropical Microcystis species. Harmful Algae 50, 88–98. https://doi.org/https://doi.org/10.1016/j.hal.2015.10.011

Müller-Navarra, D.C., Brett, M.T., Liston, A.M., Goldman, C.R., 2000. A highly unsaturated fatty acid predicts carbon transfer between primary producers and consumers. Nature 403, 74.

Neilan, B.A., Dittmann, E., Rouhiainen, L., Bass, R.A., Schaub, V., Sivonen, K.,

Börner, T., 1999. Nonribosomal peptide synthesis and toxigenicity of cyanobacteria. J. Bacteriol. 181, 4089–4097.

Neilan, B.A., Pearson, L.A., Muenchhoff, J., Moffitt, M.C., Dittmann, E., 2013. Environmental conditions that influence toxin biosynthesis in cyanobacteria. Environ. Microbiol. 15, 1239–1253. https://doi.org/10.1111/j.1462-2920.2012.02729.x

O'Neil, J.M., Davis, T.W., Burford, M.A., Gobler, C.J., 2012. The rise of harmful cyanobacteria blooms: The potential roles of eutrophication and climate change. Harmful Algae 14, 313–334. https://doi.org/10.1016/j.hal.2011.10.027

Omidi, A., Esterhuizen-Londt, M., Pflugmacher, S., 2018. Still challenging: the ecological function of the cyanobacterial toxin microcystin – What we know so far. Toxin Rev. 37, 87–105. https://doi.org/10.1080/15569543.2017.1326059

Paerl, H.W., Huisman, J., 2008. Blooms Like It Hot. Science (80-.). 320, 57 LP – 58.

Paerl, H.W., Otten, T.G., 2016. Duelling 'CyanoHABs': Unravelling the environmental drivers controlling dominance and succession among diazotrophic and non-N_2-fixing harmful cyanobacteria. Environ. Microbiol., 18:316–324. doi: 10.1111/1462-2920.13035.

Porra, R.J., Thompson, W.A., Kriedemann, P.E., 1989. Determination of accurate extinction coefficients and simultaneous equations for assaying chlorophylls a and b extracted with four different solvents: verification of the concentration of chlorophyll standards by atomic absorption spectroscopy. Biochim. Biophys. Acta - Bioenerg. 975, 384–394. https://doi.org/https://doi.org/10.1016/S0005-2728(89)80347-0

Preece, E.P., Hardy, F.J., Moore, B.C., Bryan, M., 2017. A review of microcystin detections in Estuarine and Marine waters: Environmental implications and human health risk. Harmful Algae 61, 31–45. https://doi.org/https://doi.org/10.1016/j.hal.2016.11.006

Rantala, A., Fewer, D.P., Hisbergues, M., Rouhiainen, L., Vaitomaa, J., Borner,

T., Sivonen, K., 2004. Phylogenetic evidence for the early evolution of microcystin synthesis. Proc. Natl. Acad. Sci. 101, 568–573. https://doi.org/10.1073/pnas.0304489101

Rinehart, K.L., Namikoshi, M., Choi, B.W., 1994. Structure and biosynthesis of toxins from blue-green algae (cyanobacteria). J. Appl. Phycol. 6, 159–176. https://doi.org/10.1007/BF02186070

Rippka, R., Deruelles, J., Waterbury, J.B., Herdman, M., Stanier, R.Y., 1979. Generic Assignments, Strain Histories and Properties of Pure Cultures of Cyanobacteria. Microbiology 111, 1–61. https://doi.org/10.1099/00221287-111-1-1

Rouhiainen, L., Vakkilainen, T., Siemer, B.L., Buikema, W., Haselkorn, R., Sivonen, K., 2004. Genes Coding for Hepatotoxic Heptapeptides (Microcystins) in the Cyanobacterium Anabaena Strain 90. Appl. Environ. Microbiol. 70, 686 LP – 692. https://doi.org/10.1128/AEM.70.2.686-692.2004

Rounge, T.B., Rohrlack, T., Nederbragt, A.J., Kristensen, T., Jakobsen, K.S., 2009. A genome-wide analysis of nonribosomal peptide synthetase gene clusters and their peptides in a Planktothrix rubescens strain. BMC Genomics 10, 396. https://doi.org/10.1186/1471-2164-10-396

Sandrini, G., Ji, X., Verspagen, J.M.H., Tann, R.P., Slot, P.C., Luimstra, V.M., Schuurmans, J.M., Matthijs, H.C.P., Huisman, J., 2016. Rapid adaptation of harmful cyanobacteria to rising CO_2. Proc. Natl. Acad. Sci. 113, 9315–9320. https://doi.org/10.1073/pnas.1602435113

Schatz, D., Keren, Y., Hadas, O., Carmeli, S., Sukenik, A., Kaplan, A., 2005. Ecological implications of the emergence of non-toxic subcultures from toxic Microcystis strains. Environ. Microbiol. 7, 798–805. https://doi.org/10.1111/j.1462-2920.2005.00752.x

Schopf, J.W., 1993. Microfossils of the Early Archean Apex Chert: New Evidence of the Antiquity of Life. Science (80-.). 260, 640 LP – 646.

Schuurmans, J.M., Brinkmann, B.W., Makower, A.K., Dittmann, E., Huisman, J., Matthijs, H.C.P., 2018. Microcystin interferes with defense against high

oxidative stress in harmful cyanobacteria. Harmful Algae 78, 47–55. https://doi.org/https://doi.org/10.1016/j.hal.2018.07.008

Schwarz, D., Orf, I., Kopka, J., Hagemann, M., 2013. Recent applications of metabolomics toward cyanobacteria. Metabolites 3, 72–100. https://doi.org/10.3390/metabo3010072

Shi, L., Carmichael, W.W., Miller, I., 1995. Immuno-gold localization of hepatotoxins in cyanobacterial cells. Arch. Microbiol. 163, 7–15. https://doi.org/10.1007/BF00262197

Shi, T., Falkowski, P.G., 2008. Genome evolution in cyanobacteria: The stable core and the variable shell. Proc. Natl. Acad. Sci. 105, 2510 LP – 2515.

Shishido, T.K., Kaasalainen, U., Fewer, D.P., Rouhiainen, L., Jokela, J., Wahlsten, M., Fiore, M.F., Yunes, J.S., Rikkinen, J., Sivonen, K., 2013. Convergent evolution of [D-Leucine1] microcystin-LR in taxonomically disparate cyanobacteria. BMC Evol. Biol. 13, 86. https://doi.org/10.1186/1471-2148-13-86

Sieber, S.A., Marahiel, M.A., 2005. Molecular Mechanisms Underlying Nonribosomal Peptide Synthesis: Approaches to New Antibiotics. Chem. Rev. 105, 715–738. https://doi.org/10.1021/cr0301191

Silva-Stenico, M.E., Cantúsio Neto, R., Alves, I.R., Moraes, L.A.B., Shishido, T.K., Fiore, M.F., 2009. Hepatotoxin microcystin-LR extraction optimization. J. Braz. Chem. Soc. 20, 535–542. https://doi.org/10.1590/S0103-50532009000300019

Silva-Stenico, M.E., Silva, C.S.P., Lorenzi, A.S., Shishido, T.K., Etchegaray, A., Lira, S.P., Moraes, L.A.B., Fiore, M.F., 2011. Non-ribosomal peptides produced by Brazilian cyanobacterial isolates with antimicrobial activity. Microbiol. Res. 166, 161–175. https://doi.org/https://doi.org/10.1016/j.micres.2010.04.002

Silva, C.S.P., Genuário, D.B., Vaz, M.G.M.V., Fiore, M.F., 2014. Phylogeny of culturable cyanobacteria from Brazilian mangroves. Syst. Appl. Microbiol. 37, 100–112. https://doi.org/10.1016/j.syapm.2013.12.003

Smith, V.H., Tilman, G.D., Nekola, J.C., 1999. Eutrophication: Impacts of excess nutrient inputs on freshwater, marine, and terrestrial ecosystems. Environ. Pollut., 100:179–196. doi: 10.1016/S0269-7491(99)00091-3.

Sivonen, K., Jones, G., 1999. Chapter 3. CYANOBACTERIAL TOXINS, in: Bartram, J., Chorus, I. (Eds.), Toxic Cyanobacteria in Water: A Guide to Their Public Health Consequences, Monitoring and Management. London, p. 432.

Stachelhaus, T., Mootz, H.D., Marahiel, M.A., 1999. The specificity-conferring code of adenylation domains in nonribosomal peptide synthetases. Chem. Biol. 6, 493–505. https://doi.org/https://doi.org/10.1016/S1074-5521(99)80082-9

Tchernov, D., Silverman, J., Luz, B., Reinhold, L., Kaplan, A., 2003. Massive light-dependent cycling of inorganic carbon between oxygenic photosynthetic microorganisms and their surroundings. Photosynth. Res. 77, 95–103. https://doi.org/10.1023/A:1025869600935

Tillett, D., Dittmann, E., Erhard, M., von Döhren, H., Börner, T., Neilan, B.A., 2000. Structural organization of microcystin biosynthesis in Microcystis aeruginosa PCC7806: an integrated peptide–polyketide synthetase system. Chem. Biol. 7, 753–764. https://doi.org/10.1016/S1074-5521(00)00021-1

Touloupakis, E., Cicchi, B., Benavides, A.M.S., Torzillo, G., 2016. Effect of high pH on growth of Synechocystis sp. PCC 6803 cultures and their contamination by golden algae (Poterioochromonas sp.). Appl Microbiol Biotechnol, 100:1333–1341 DOI 10.1007/s00253-015-7024-0

Van De Waal, D.B., Verspagen, J.M.H., Finke, J.F., Vournazou, V., Immers, A.K., Kardinaal, W.E.A., Tonk, L., Becker, S., Van Donk, E., Visser, P.M., Huisman, J., 2011. Reversal in competitive dominance of a toxic versus non-toxic cyanobacterium in response to rising CO2. ISME J. 5, 1438–1450. https://doi.org/10.1038/ismej.2011.28

van der Westhuizen, A.J., Krüger, G.H.J., Eloff, J.N., 1988. Effect of culture age and pH of the culture medium on the composition of the toxin of the cyanobacterium Microcystis aeruginosa (UV-006). South African J. Bot. 54,

372–374. https://doi.org/https://doi.org/10.1016/S0254-6299(16)31304-7

Vasconcelos, V., 2006. Eutrophication, toxic cyanobacteria and cyanotoxins: when ecosystems cry for help. Limnetica, 25(1-2): 425-432. The ecology of the Iberian inland waters: Homage to Ramon Margalef © Asociación Española de Limnología, Madrid. Spain. ISSN: 0213-8409

Walsh, C.T., Chen, H., Keating, T.A., Hubbard, B.K., Losey, H.C., Luo, L., Marshall, C.G., Miller, D.A., Patel, H.M., 2001. Tailoring enzymes that modify nonribosomal peptides during and after chain elongation on NRPS assembly lines. Curr. Opin. Chem. Biol. 5, 525–534. https://doi.org/https://doi.org/10.1016/S1367-5931(00)00235-0

Watanabe, M.F., Oishi, S., Harada, K.-I., Matsuura, K., Kawai, H., Suzuki, M., 1988. Toxins contained in Microcystis species of cyanobacteria (blue-green algae). Toxicon 26, 1017–1025. https://doi.org/https://doi.org/10.1016/0041-0101(88)90200-0

Watson, S.B., McCauley, E., Downing, J.A., 1997. Patterns in phytoplankton taxonomic composition across temperate lakes of differing nutrient status. Limnol. Oceanogr., 42:487–495. doi: 10.4319/lo.1997.42.3.0487.

Watson, S.B., 2003. Cyanobacterial and eukaryotic algal odour compounds: signals or by-products? A review of their biological activity. Phycologia 42, 332–350. https://doi.org/10.2216/i0031-8884-42-4-332.1

Woese, C.R., 1987. Bacterial evolution. Microbiol. Rev. 51, 221 LP – 271.

Xu, Y., Tiago Guerra, L., Li, Z., Ludwig, M., Charles Dismukes, G., Bryant, D.A., 2013. Altered carbohydrate metabolism in glycogen synthase mutants of Synechococcus sp. strain PCC 7002: Cell factories for soluble sugars. Metab. Eng. 16, 56–67. https://doi.org/https://doi.org/10.1016/j.ymben.2012.12.002

Young, F.M., Morrison, L.F., James, J., Codd, G.A., 2008. Quantification and localization of microcystins in colonies of a laboratory strain of Microcystis (Cyanobacteria) using immunological methods. Eur. J. Phycol. 43, 217–225. https://doi.org/10.1080/09670260701880460

Yu, L., Kong, F., Zhang, M., Yang, Z., Shi, X., Du, M., 2014. The dynamics of

microcystis genotypes and microcystin production and associations with environmental factors during blooms in Lake Chaohu, China. Toxins (Basel). 6, 3238–3257. https://doi.org/10.3390/toxins6123238

Zhang, C.-C., Zhou, C.-Z., Burnap, R.L., Peng, L., 2018. Carbon/Nitrogen Metabolic Balance: Lessons from Cyanobacteria. Trends Plant Sci. 23, 1116–1130. https://doi.org/10.1016/j.tplants.2018.09.008

Zhang, Y., Jiang, H.-B., Liu, S.-W., Gao, K.-S., Qiu, B.-S., 2012. Effects of dissolved inorganic carbon on competition of the bloom-forming cyanobacterium Microcystis aeruginosa with the green alga Chlamydomonas microsphaera. Eur. J. Phycol. 47, 1–11. https://doi.org/10.1080/09670262.2011.645073

Zhen, Y., Kong, F., 2012. Formation of large colonies: A defense mechanism of Microcystis aeruginosa under continuous grazing pressure by flagellate Ochromonas sp. J. Limnol. 71, 61–66. https://doi.org/10.3274/JL12-71-1-02

Zilliges, Y., Kehr, J.-C., Meissner, S., Ishida, K., Mikkat, S., Hagemann, M., Kaplan, A., Börner, T., Dittmann, E., 2011. The Cyanobacterial Hepatotoxin Microcystin Binds to Proteins and Increases the Fitness of Microcystis under Oxidative Stress Conditions. PLoS One 6, e17615.

8. SUPPLEMENTAL MATERIAL

8.1 Supplemental Tables

Supplemental table S1: Statistical analysis of the growth curve during 15 days (Figure 3).

Days/Treatments	Control	T1	T2	T3
0	-2.35**b**	-2.29**b**	-1.95**a**	-2.32**b**
1	-1.99**a**	-2.05**a**	-2.01**a**	-2.36**b**
2	-1.89**a**	-1.83**a**	-1.85**a**	-2.17**b**
3	-1.72**b**	-1.49**a**	-1.62**b**	-1.87**c**
4	-1.51**a**	-1.34**a**	-1.38**a**	-1.84**b**
5	-1.25**b**	-0.98**a**	-1.25**b**	-1.55**c**
6	-1.06**a**	-1.02**a**	-1.13**a**	-1.37**b**
7	-1.04**ab**	-0.91**a**	-1.11**bc**	-1.24**c**
8	-0.98**b**	-0.65**a**	-0.93**b**	-0.96**b**
9	-0.82**b**	-0.58**a**	-0.84**b**	-0.93**b**
10	-0.81**a**	-0.62**a**	-0.84**a**	-0.77**a**
11	-0.62**a**	-0.79**a**	-0.79**a**	-0.76**a**
12	-0.61**a**	-0.57**a**	-0.69**a**	-0.65**a**
13	-0.60**a**	-0.65**a**	-0.52**a**	-0.50**a**
14	-0.51**a**	-0.45**a**	-0.50**a**	-0.57**a**

Different letters represent average values between treatments that were judged to be statistically different ($P < 0.05$, Tukey test).

Supplemental table S2: Statistical analysis of the growth curves based on Ln (OD_{750nm}) monitored at 6 hours' intervals during 24 hours in two growth phases (Figure 4).

Log phase				
Hours/ Treatment	Control	T1	T2	T3
0	-1.45**Bc**	-1.05**Aa**	-1.62**Bc**	-1.35**ABa**
6	-1.41**Cbc**	-1.32**Ba**	-1.52**Dbca**	-1.14**Aa**
12	-1.34**ABbc**	-1.30**ABa**	-1.48**Bbc**	-1.17**Aa**
18	-1.16**Aa**	-1.03**Aa**	-1.20**Aab**	-0.99**Aa**
24	-1.29**Aab**	-1.19**Aa**	-1.37**Aab**	-1.17**Aa**

Stationary phase				
Hours/ Treatment	Control	T1	T2	T3
0	-0.73**BCa**	-0.64**Ba**	-0.83**Ca**	-0.52**Aa**
6	-0.70**BCa**	-0.61**Ba**	-0.80**Ca**	-0.40**Aa**
12	-0.67**BCa**	-0.62**Ba**	-0.78**Ca**	-0.38**Aa**
18	-0.63**BCa**	-0.57**ABa**	-0.80**Ca**	-0.38**Aa**
24	-0.76**Ba**	-0.56**ABa**	-0.73**Ba**	-0.43**Aa**

Different letters represent average values that were judged to be statistically different ($P < 0.05$, Tukey test). Capital letters represent statistical differences between the treatments, and lower-case letters demonstrate statistical differences along time.

Supplemental table S3: Statistical analysis of the growth curves based ash-free dry mass monitored at 6 hours' intervals during 24 hours in two growth phases. (Figure 5).

Log phase				
Hours/ Treatment	Control	T1	T2	T3
0	0.23**Ba**	0.17**Bb**	0.05**Bb**	0.43**Ab**
6	0.14**Bb**	0.22**Bb**	0.08**Bb**	0.43**Ab**
12	0.17**Bab**	0.25**Bab**	0.16**Bb**	0.46**Ab**
18	0.19**Bab**	0.44**Aa**	0.12**Bb**	0.60**Aa**
24	0.20**BCab**	0.31**Bab**	0.11**Ca**	0.55**Aab**

Stationary phase				
Hours/ Treatment	Control	T1	T2	T3
0	0.65**Db**	0.57**Bb**	0.38**Cb**	0.86**Aa**
6	0.53**Ba**	0.49**Bb**	0.41**Bab**	0.96**Aa**
12	0.59**Ba**	0.59**Bb**	0.46**Bab**	1.03**Aa**
18	0.53**Ca**	0.81**Ba**	0.42**Cab**	0.98**Aa**
24	0.56**Ba**	0.56**Bb**	0.49**Ba**	0.96**Aa**

Different letters represent average values that were judged to be statistically different ($P < 0.05$, Tukey test). Capital letters represent statistical differences between the treatments, and lower-case letters demonstrate statistical differences along time.

Supplemental table S4: Statistical analysis of the photosynthesis rate monitored at 6 hours' intervals during 24 hours in two growth phases. Figure 7A and 8A.

Log phase				
Hours/ Treatment	Control	T1	T2	T3
0	0.80**Bc**	3.12**Bb**	12.29**Aa**	6.78**ABa**
6	4.98**Ab**	6.41**Ba**	5.68**Aab**	4.98**Aa**
12	11.07**Aa**	12.28**Aa**	3.12**Bb**	4.86**Ba**

Stationary phase				
Hours/ Treatment	Control	T1	T2	T3
0	2.35**Bb**	1.82**Bb**	0.94**Bb**	13.35**Aa**
6	1.92**Bb**	0.70**Bb**	11.33**Aa**	8.08**Aa**
12	4.58**Aa**	8.02**Aa**	7.96**Aa**	7.97**Aa**

Different letters represent average values that were judged to be statistically different ($P < 0.05$, Tukey test). Capital letters represent statistical differences between the treatments, and lower-case letters demonstrate statistical differences along time.

Supplemental table S5: Statistical analysis of the respiration rates monitored at 6 hours' intervals during 24 hours in two growth phases. Figure 7B and 8B.

Log phase				
Hours/ Treatment	Control	T1	T2	T3
0	-0.46**Aa**	-0.54**Aa**	-3.84**Bc**	-4.28**Ba**
6	-1.73**Aa**	-1.69**Aab**	-3.00**Bbc**	-4.93**CB**
12	-6.74**Bb**	-3.04**Abc**	-1.22**Aab**	-5.65**Bb**
18	-7.25**Cb**	-4.08**Bc**	-1.14**Aab**	-3.80**Bab**
24	-6.52**Bb**	-2.88**Abc**	-0.91**Aa**	-2.64**Aa**

Stationary phase				
Hours/ Treatment	Control	T1	T2	T3
0	-0.57**Ba**	-0.49**Ba**	-0.23**Ba**	-3.38**Aab**
6	-1.38**Aab**	-0.49**Aa**	-3.31**Bb**	-3.86**Bb**
12	-3.50**Ac**	-2.0**Abc**	-3.19**Ab**	-3.27**Aab**
18	-1.55**Aab**	-1.5**Ab**	-1.22**Aa**	-2.90**Bab**
24	-2.10**Aab**	-2.01**Ac**	-1.27**Aa**	-2.05**Aa**

Different letters represent average values that were judged to be statistically different ($P < 0.05$, Tukey test). Capital letters represent statistical differences between the treatments, and lower-case letters demonstrate statistical differences along time.

8.2 Supplemental figures

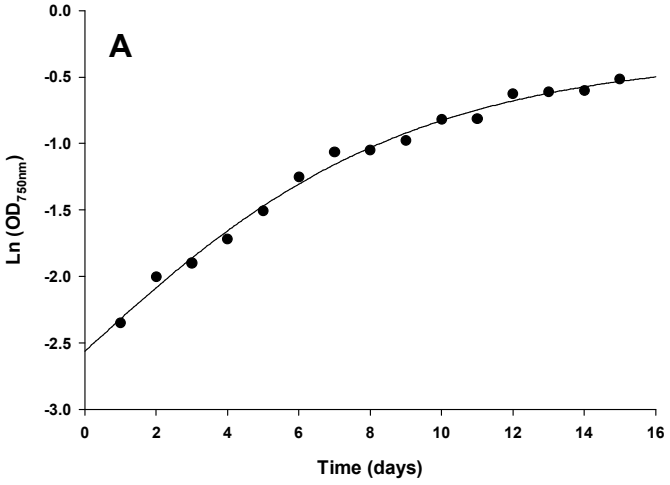

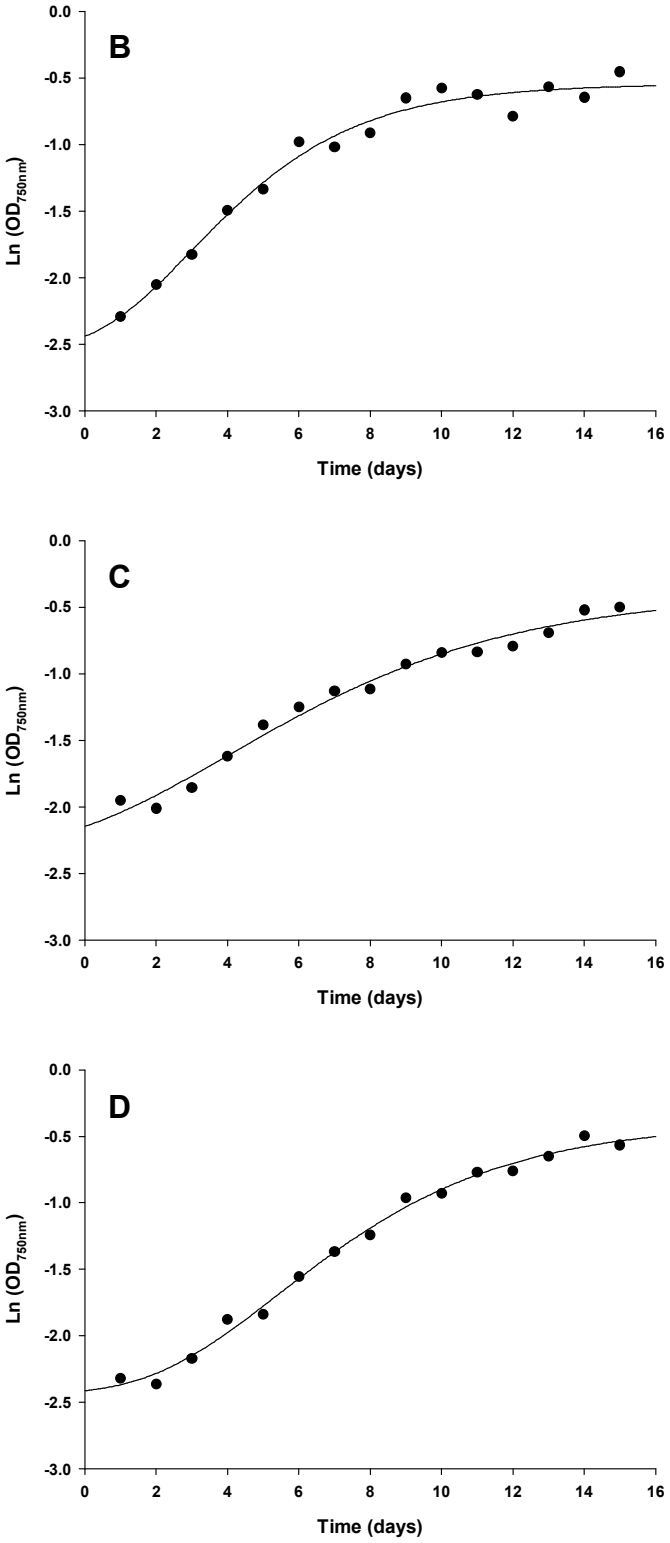

Supplemental figure S1. Growth curves based on optical density measurements (OD_{750nm}). Growth was monitored at 24 hours' intervals during 15 days. **(A)** Control, BG-11_0 medium with 0.02 g·L-^{1} of sodium carbonate; **(B)** T1, BG-11_0 medium without any source of carbon; **(C)** T2, BG-11_0 medium with 0.016 g·L^{-1} of sodium bicarbonate; **(D)** T3, BG-11_0 medium with 1.6 g·L^{-1} of

sodium bicarbonate. Values represent trend curves obtained from means ± standard error (n = 4).

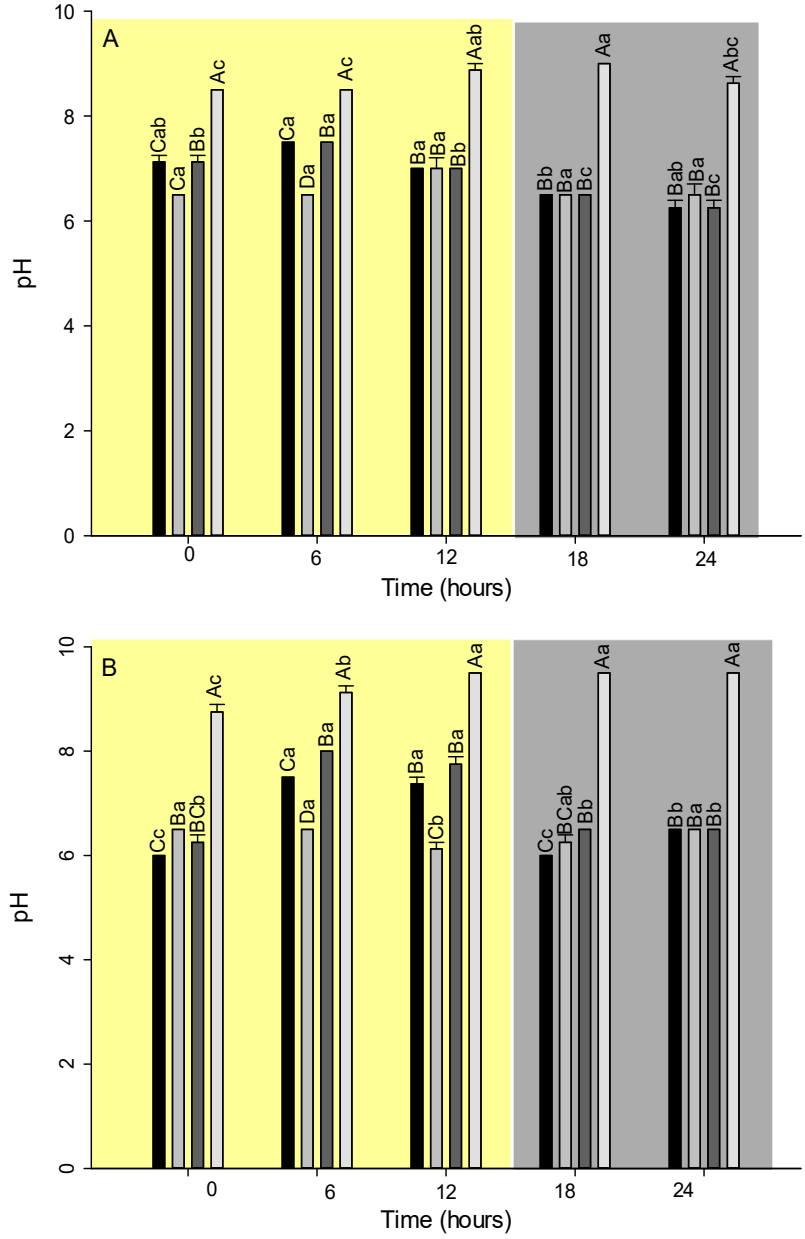

Supplemental figure S2. Variation of pH values. The pH values were measured at 6 hours' intervals during 24 hours using pH tapes. **(A)** Log phase; **(B)** Stationary phase. Treatments: Control (black bars): BG-11_0 culture medium supplied with 0.02 g·L^{-1} of sodium carbonate; T1 (light grey bars): BG-11_0 culture medium without carbon source carbon; T2 (dark grey bars): BG-11_0 medium with 0.016 g·L^{-1} of sodium bicarbonate; T3 (lighter grey bars) BG-11_0 medium with 1.6 g·L^{-1} of sodium bicarbonate. Values are presented as means ± error (n=4). Different letters represent average values that were judged to be statistically different (P < 0.05, Tukey test). Capital letters represent statistical differences between the treatments, and lower-case letters demonstrate statistical differences along time.